USGS
science for a changing world

Coastal Circulation and Sediment Dynamics in Maunalua Bay, Oahu, Hawaii

Measurements of Waves, Currents, Temperature, Salinity, and Turbidity: **November 2008—February 2009**

By Curt D. Storlazzi, M. Katherine Presto, Joshua B. Logan, and Michael E. Field

Open-File Report 2010-1217

U.S. Department of the Interior
U.S. Geological Survey

U.S. Department of the Interior
KEN SALAZAR, Secretary

U.S. Geological Survey
Marcia K. McNutt, Director

U.S. Geological Survey, Reston, Virginia: 2010

For product and ordering information:
World Wide Web: *http://www.usgs.gov/pubprod*
Telephone: 1-888-ASK-USGS

For more information on the USGS—the Federal source for science about the Earth, its natural and living resources, natural hazards, and the environment:
World Wide Web: *http://www.usgs.gov*
Telephone: 1-888-ASK-USGS

Suggested citation:
Storlazzi, C.D., Presto, M.K., Logan, J.B., and Field, M.E., 2010, Coastal circulation and sediment dynamics in Maunalua Bay, Oahu, Hawaii; measurements of waves, currents, temperature, salinity, and turbidity; November 2008-February 2009: U.S. Geological Survey Open-File Report 2010-1217, 59 p. [*http://pubs.usgs.gov/of/2010/1217/*].

Contents

Figures

Tables

Coastal Circulation and Sediment Dynamics in Maunalua Bay, Oahu, Hawaii

Measurements of Waves, Currents, Temperature, Salinity, and Turbidity: November 2008—February 2009

By Curt D. Storlazzi, M. Katherine Presto, Joshua B. Logan, and Michael E. Field

Introduction

High-resolution measurements of waves, currents, water levels, temperature, salinity and turbidity were made in Maunalua Bay, southern Oahu, Hawaii, during the 2008-2009 winter to better understand coastal circulation, water-column properties, and sediment dynamics during a range of conditions (trade winds, kona storms, relaxation of trade winds, and south swells). A series of bottom-mounted instrument packages were deployed in water depths of 20 m or less to collect long-term, high-resolution measurements of waves, currents, water levels, temperature, salinity, and turbidity. These data were supplemented with a series of profiles through the water column to characterize the vertical and spatial variability in water-column properties within the bay. These measurements support the ongoing process studies being done as part of the U.S. Geological Survey (USGS) Coastal and Marine Geology Program's Pacific Coral Reef Project; the ultimate goal of these studies is to better understand the transport mechanisms of sediment, larvae, pollutants, and other particles in coral reef settings.

Project Objectives

The objective of this study was to understand the temporal variations in currents, waves, tides, temperature, salinity and turbidity within a coral-lined embayment that receives periodic discharges of freshwater and sediment from multiple terrestrial sources in the Maunalua Bay. Instrument packages were deployed for a three-month period during the 2008-2009 winter and a series of vertical profiles were collected in November 2008, and again in February 2009, to characterize water-column properties within the bay. Measurements of flow and water-column properties in Maunalua Bay provided insight into the potential fate of terrestrial sediment, nutrient, or contaminant delivered to the marine environment and coral larval transport within the embayment. Such data are useful for providing baseline information for future watershed decisions and for establishing guidelines for the U.S. Coral Reef Task Force's (USCRTF) Hawaiian Local Action Strategy to address Land-Based Pollution (LAS-LBP) threats to coral reefs adjacent to the urbanized watersheds of Manualua Bay.

Study Area

Maunalua Bay is on the south side of Oahu, Hawaii (fig. 1), and is approximately 10 km long and 3 km wide. The bay is flanked by two large, dormant craters: Koko Head to the east and Diamond Head to the west. Rainfall in the watersheds that drain into Maunalua Bay ranges from more than 200 cm/year at the top of the Ko'olau Range that borders the northwestern part of the bay to less than 70 cm/year to the east at Koko Head. Seven major channels flow into the bay, and all but one have been altered by engineering structures.

Operations

This section provides information about the personnel, equipment, and field operations used during the study. See table 1 for a list of personnel involved in the experiment and tables 2 through 14 for complete listings of instrument and deployment information.

The study consisted of three suites of instruments to provide an integrated understanding of circulation and sediment dynamics in Maunalua Bay's coastal waters: terrestrial instruments, bottom-mounted oceanographic instruments, and spatial hydrographic surveys. The terrestrial instruments included a weather station and a digital-camera system. These were deployed on top of the Mt. Terrace Apartments in Hawaii Kai to get a wide field of view of the bay and un-obstructed meteorologic data (fig. 1). The bottom-mounted oceanographic instruments were deployed in two reef-parallel alongshore arrays along the 10 m and 20 m isobaths. In addition to these fixed, bottom-mounted, time-series measurements, repetitive surveys of water-column properties were made in various locations throughout the bay at the beginning (November 2008) and end (February 2009) of the experiment. All vessel operations, including mobilization and demobilization, were based out of Ala Wai marina approximately 5 km to the east of the bay, and all instrument packages were situated on the sandy seabed in water depths less than 20 m.

Equipment and Data Review

Acoustic Doppler Current Profilers (ADCP)

Six upward-looking acoustic Doppler current profilers (ADCP) were mounted on MiniPROBEs (MP) packages (fig. 2*A*) along the 10 m and 20 m isobaths in Maunalua Bay. These ADCPs sampled 0.5-m vertical bins from 1.0 m above the seafloor up to the surface for 180 s at 2 Hz every 10 min to allow calculation of tides from modulations in water level (m), mean current speeds (m/s), mean current directions (°True), and higher frequency motions such as internal tidal bores and non-linear internal waves. Directional wave data were recorded for 1,024 s at 2 Hz every two hours; these data included significant wave height (m), dominant wave period (s), mean wave direction (°True), and directional spread (°). Acoustic backscatter data (dB) collected from the ADCPs for the current measurements also provide information on the particulates in the water column and are used as a qualitative measurement of turbidity. The sensor locations are listed in tables 2 and 3; complete sensor and processing information is listed in appendix 1.

Conductivity and Temperature (CT)

Seven conductivity and temperature (CT) sensors (fig. 2*A*) also were mounted on the MPs and collected and averaged 4 samples every 5 min to measure water temperature (°C) and conductivity (S/m), from which salinity (PSU) was calculated. The rapid sampling rate was used in an attempt to record any transient freshwater plumes and/or submarine groundwater discharge being advected past the instruments. Offshore instrument locations were selected to record the distance, mixing, and direction of freshwater with oceanic water and to correlate with current measurements. The sensor locations are listed in tables 2 and 3; complete sensor and processing information is listed in appendix 2.

Turbidity Sensors (SLOBS)

Eight self-logging optical backscatter sensors (SLOBS; fig. 2*A*) averaged 8 samples every 5 min to measure turbidity data in Nephelometric Turbidity Units (NTU). The SLOBS were calibrated to suspended-sediment concentrations (SSC) in mg/L using seafloor sediment from the bay. The SLOBS on the MPs were mounted above the ADCPs in order for the turbidity data to be correlated with the along- and cross-shore velocity data from the bin closest to the seabed of the ADCPs to calculate

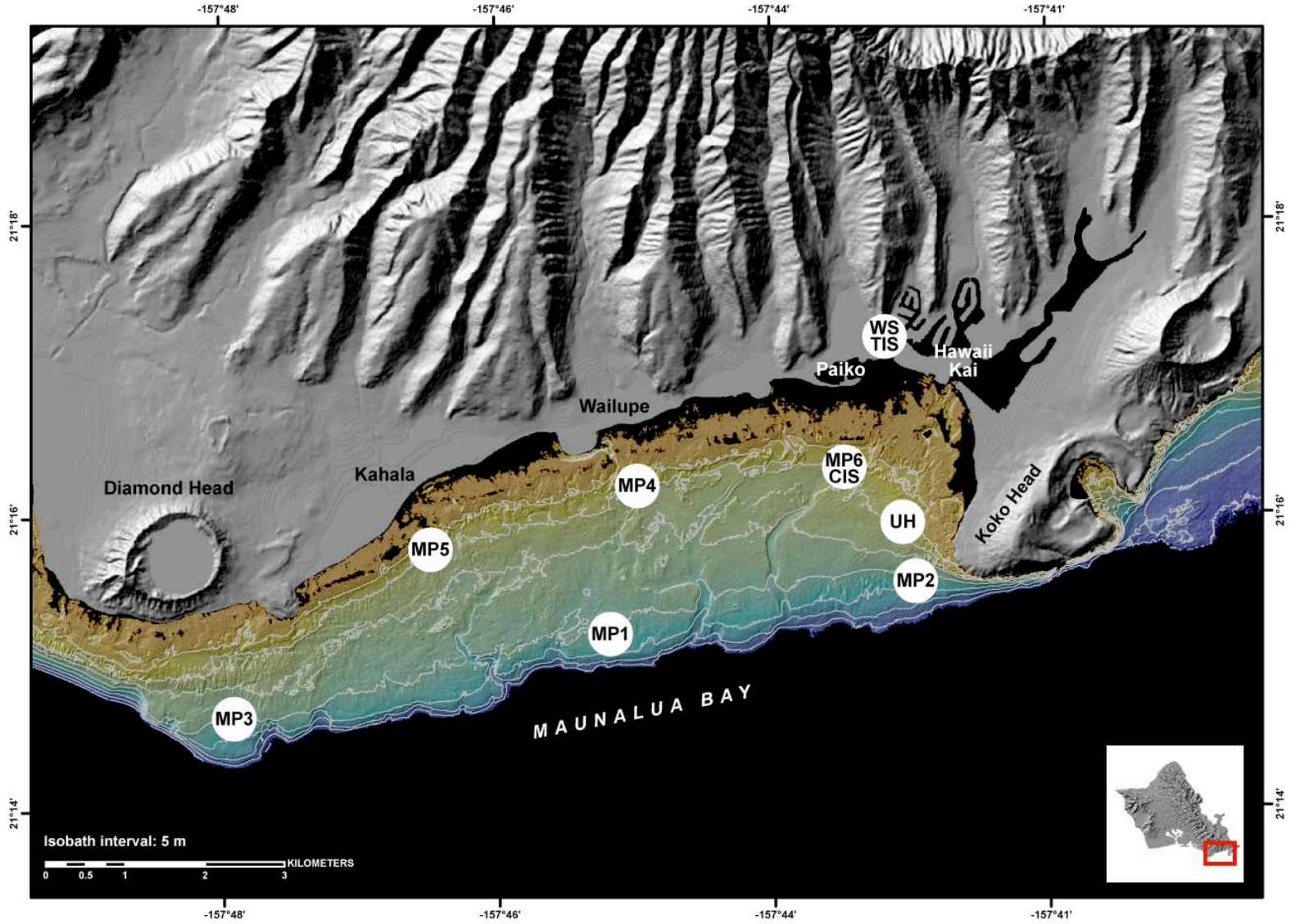

FIGURE 1. Terrestrial digital elevation model (DEM) and SHOALS lidar of Maunalua Bay and its location on Oahu, Hawaii. White dots denote the location of instrument packages; see table 2 for more information on the instrument packages.

sediment flux. The sensor locations are listed in tables 2 and 3; complete sensor information is listed in appendix 2, and calibration information is listed in appendix 7.

Weather Station (WS)

Meteorological data were acquired by a self-contained weather station (WS) deployed on top Mt. Terrace Apartments (fig. 1,2*B*), 71 m above ground, in the northeast corner of the bay. The WS recorded 25 min averages of barometric pressure (mb), air temperature (°C), precipitation (mm), wind speed (m/s), and wind direction (°True) every half hour. The instrument's location is listed in table 3; complete sensor information is listed in appendix 3.

Terrestrial Imaging System (TIS)

Imagery of Maunalua Bay was collected using the USGS Terrestrial Imaging System (TIS), which consists of a Nikon CoolPix 8700 8-megapixel digital camera, a control unit, and battery in a waterproof housing with an external solar panel (fig. 2*C*). The TIS was mounted on a metal pole that was attached to the top of the apartment building at an elevation of approximately 70 m above sea level to achieve an unobstructed view of the eastern half of the bay. This system was employed to collect a time series of images to provide information on the natural frequency and duration of processes impacting the Bay (stream discharge, freshwater, sediment plumes, storms and waves). The TIS took images approximately every two hours during daylight hours (06:00, 07:00, 08:00, 10:00, 12:00, 14:00, 16:00, and 18:00 HST) throughout the deployments. The sensor location is listed in tables 2 and 3; complete sensor information is listed in appendix 3.

Water Column Profiler (WCP)

Vessel-based surveys of water-column properties were made using a Conductivity/Temperature/Depth (CTD) Profiler with Optical Backscatter (OBS), Photosynthetically-Available Radiation (PAR) Sensor, Dissolved Oxygen (DO) sensor, and a fluorometer that measured chlorophyll (chl) . This package collected vertical profiles of water temperature (°C), salinity (PSU), density (kg/m^3), turbidity (NTU), PAR (mE), DO (%), and chl (mg/m^3), as shown in figure 2*D*. The profiler data position and depth information is listed in table 4; complete sensor information and individual cast acquisition logs are listed in appendixes 4-7. The profile surveys were completed during approximately 3-hour periods between Koko Head and Diamond Head craters at the beginning and end of the deployment (November 2008 and February 2009).

Coral Imaging System (CIS)

The USGS Coral Imaging System (CIS) was used to collect a time series of seabed images and consists of a Canon D60 6.3-megapixel digital camera with a 24-mm lens, an external Canon Speedlight 550EX TTL strobe, control unit and batteries all mounted on a tetrapod (fig. 2*E*), it was used to collect a time series of seabed images. The CIS was deployed in a patch of sand at the MP6 site, and the camera and strobe were angled to not only record images of the adjacent reef, but also of a gridded black and white camera-calibration reference block. The CIS provided data on the natural frequency and duration of sediment deposition and resuspension on an actual coral surface. The CIS took images every four hours throughout the deployment (0000, 0400, 0800, 1200, 1600, and 2000 HST); complete sensor information is listed in appendix 3.

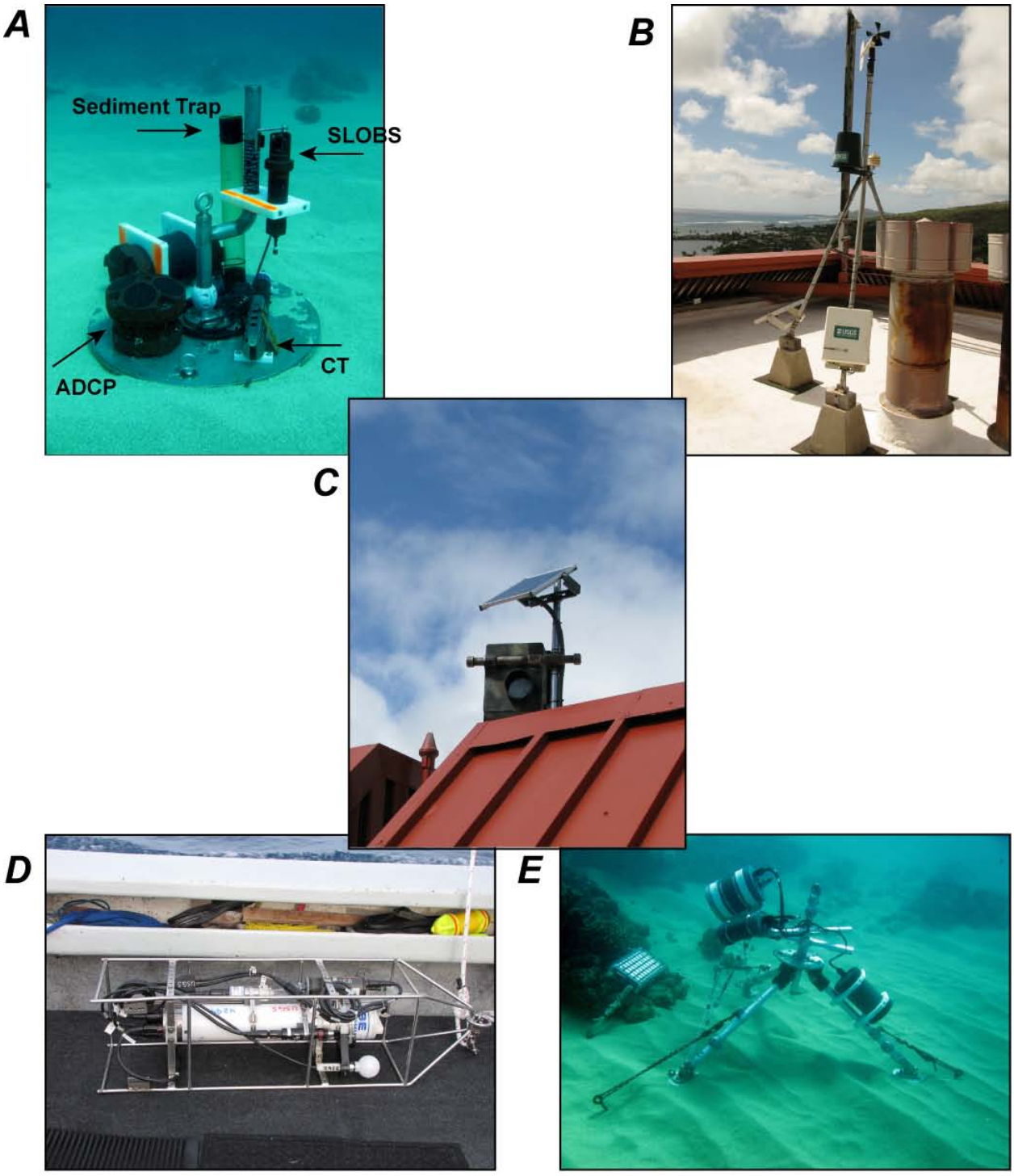

FIGURE 2. Photographs of the equipment used in the study. *A*, Example of a MiniProbe with Acoustic Doppler Current Profiler (ADCP), Self-Logging Optical Backscatter Sensor (SLOBS), Conductivity and Temperature sensor (CT), and sediment tube trap along the 20 m isobath at site MP2. *B*, Weather Station (WS) on the Mt. Terrace Apartments. *C*, Terrestial Imaging System (TIS) on the Mt. Terrace Apartments. *D*, Water Column Profiler (WCP). *E*, Coral Imaging System (CIS).

Sediment Data

Sediment traps were deployed during the entire length of the experiment (November 2008-February 2009) at all six MP sites to collect suspended sediment from the water column. Simple tube traps, consisting of a clear plastic tube 60 cm long with an internal diameter of 6.7 cm, were deployed with their openings 0.7 m above the seabed at the six main instrument sites. A baffle was placed in the top of each tube trap to reduce turbulence and minimize disturbance by aquatic organisms (Bothner and others, 2006), as shown in figure 2*A*. Net vertical sediment flux onto the coral reef surface was not measured by the sediment traps due to the energetic nature of the deployment sites on the inner shelf, principally because material falling into the trap has a much lower potential for resuspension than the same material that settles on the adjacent reef surface (Bothner and others, 2006). Coarse sediment particles likely were collected preferentially because of their higher settling velocity than finer particles. Thus finer particles with slow settling velocities relative to the circulation and exchange of water contained in the trap can be underrepresented in the collected samples (for example, Gardner and others, 1983; Baker and others, 1988). The location and depth of each sediment trap is listed in table 11. In addition to these suspended-sediment samples, seabed-sediment samples were collected by divers at the MP study sites. The bulk grain sizes of the seabed and sediment-trap samples were analyzed using both Beckman Coulter Counter (silt and clay fractions) and 2-m settling tubes (sand fraction), and within each grain size fraction the percentage of carbonate was determined with a UIC Coulometer. Carbonate and terrigenous percentages for the sand-, silt-, and clay-size fractions were determined using the methodology developed by Barber (2002).

Miscellaneous Data Sources

Discharge data (m^3/s) for the H-1 storm drain at Kapiolani Avenue were provided by the National Water Information System's stream-flow gauge #211722157485601 (NWIS, 2010); listed in table 3. Navigation equipment for deployment, recovery, and survey operations included a hand-held WAAS-equipped GPS unit and a computer with positioning and mapping software. The positioning and mapping software enabled real-time GPS position data to be combined with images of previously collected high-resolution SHOALS color-coded LiDAR, shaded-relief bathymetry, 5-m isobaths, and aerial photographs of terrestrial portions of the maps.

Research Platform and Field Operations

The instrument deployments and recoveries were done using the *F/V Alyce C*. Vessel operations, including mobilization and demobilization, were based out of the Ala Wai marina, Oahu, Hawaii. The port quarterdeck was adapted for instrument deployment and recovery operations, which included the use of an electric winch and an overhead davit. The instruments were deployed by attaching a removable bridle to the instrument package with a connecting line through the davit and down to the winch. The instruments were lowered to within a few meters of the seafloor where scuba divers attached a lift bag and detached the lifting line. The divers then moved the instrument package into position for anchoring. Surficial seafloor sediment samples were collected, and the heights of the sensors above the seafloor were measured and recorded. Recovery operations employed the same techniques. The WCP casts were done by hand from the same vessel. The vessel wheelhouse was outfitted with a laptop computer and GPS-enabled navigation system to provide the vessel captain with a graphic display of position information, speed, heading, and distance to the next location.

Data Acquisition and Quality

Data were acquired for 98 days during the period between November 10, 2008, and February 15, 2009 (2008 Year Day [YD] 315-413). More than 2.6 million data points were recorded by the ADCPs,

CTs, SLOBS, and WS, more than 12,000 data points were recorded by the WCP, 648 images were taken by the TIS, and 192 images were taken by the CIS. The raw data were archived and copies of the data were post-processed for analysis.

The ADCP, CT, SLOBS, TIS, and WS data generally appeared to be of high quality. The ADCP at site MP6 stopped recording on 2008 Year Day 388 due to an electronic malfunction. The SLOBS at sites MP2, MP3, and UH had issues with their anti-biofouling wipers and thus reliable data were recorded only for the first 11 days of the experiment (2008 Year Days 315-325). The CTs had intermittent anomalously low conductivity (and thus salinity) values during large wave events when sediment clogged the conductivity cell.

The ADCPs' current data were 10-28 hour band-pass filtered to investigate the contribution of the tides to flow patterns and 36 hour low-pass filtered to look at the influence of winds and waves when one or the other was the primary forcing condition (for example, weak winds and large waves or strong winds and small waves). In order to address sediment fluxes in the bay, we computed suspended-sediment concentrations in mg/L for the SLOBS as addressed above. The CIS imagery, although overall very good at the beginning of the deployment, was inoperable after a Kona storm on December 11, 2008, damaged the camera. The WCP data were high in quality; however, as typically occurs, the OBS data near the surface and seabed often displayed spikes due to interaction of the optical beam with the vessel or the seabed, respectively. These spurious profiler data were removed during processing. Electronic issues with the WCP's PAR sensor made the data unreliable and, therefore, these data are not presented in this report.

Results

This section reviews the data collected by the instruments during the deployments and addresses the significance of the findings to better understand the oceanographic conditions in the study area.

Oceanographic and Atmospheric Forcing

The study period from November 2008 through February 2009 covered the beginning of the wet, non-trade wind season in Hawaii (fig. 3). The precipitation ranged from 0.0 to 10.3 mm/30 min, with a mean rainfall ± one standard deviation of 0.1±0.4 mm/30 min (fig. 3e). The majority of precipitation occurred during storms approaching from the south, with some of the precipitation due to orographic effects associated with strong trade winds blowing over the Ko'olau Range. The air temperature ranged from 17.75 to 29.31ºC with a mean temperature ± one standard deviation of 22.97±1.55ºC (fig. 3b). Diurnal heating on the order of 1 to 2ºC was observed, with a slight decrease caused by the seasonal trend in temperature during the course of the deployment corresponding to the onset of the northern hemisphere winter.

Stream Discharge

Daily stream-discharge data were acquired from the USGS stream-flow gauge in the H-1 storm drain at Kapiolani Avenue, Oahu, Hawaii (fig. 3*F*). These data provide a measure of the stream response to precipitation in the study area. Discharge ranged from 0 to 0.21 m^3/s, with a mean discharge ± one standard deviation of 0.0047±0.02 m^3/s. The highest discharge coincided with the heavy precipitation from December 11, 2008, through December 15, 2008, (2008 YD 346-350; fig. 3*E*,*F*).

Winds

The mean wind speeds at the WS in Maunalua Bay ranged from 0.00 to 15.75 m/s, with a mean speed ± one standard deviation of 4.77±2.83 m/s during the deployment (fig. 3*C*). The mean wind

direction ± one standard deviation during the deployment was 105.2±84.7° (fig. 3*D*). Winds predominantly from the east were classified as "trade winds" and were associated with dry, stable weather; this set of forcing conditions characterized approximately 50 percent of the study period. Strong, south winds were associated with drops in barometric pressure from locally generated storms that usually coincided with rainfall. Light, variable winds also are prevalent during this deployment and were associated with low amounts of rainfall and stable weather patterns.

Waves

The waves that impacted Maunalua Bay during the course of the experiment measured by the directional wave gauge at the MP1 site in the central part of the bay are shown in fig. 4. Significant wave heights ranged from 0.48 to 4.07 m, with a mean significant height ± one standard deviation of 1.06±0.34 m (fig. 4*A*,*B*). Dominant wave periods varied from 2.2 to 6.7 s, with a mean dominant period ± one standard deviation of 4.4±0.6 s (fig. 4*C*). The mean wave direction ± one standard deviation was 146.1±17.2°. The waves measured at the MP1 site were consistently from the southeast with wave heights and periods on the order of 1 m and 4 s, respectively, that were generated by the strong easterly trade winds. A large south swell (>4m) was measured from December 10-15, 2008 (2008 YD 344-349), during the large Kona storm that impacted Maunalua Bay. This swell coincided with strong winds and a large amount of precipitation during a short period of time. Wave heights at the shallow sites (MP4-6, depth <10 m) show similar patterns but are smaller in size than the deep sites (depths ~20 m).

Tides

The study period encompassed more than seven complete spring-neap tidal cycles (fig. 5*A*). Tides in Maunalua Bay are typical for the Hawaiian Islands: microtidal, mixed, semi-diurnal with two uneven high tides and two uneven low tides per day, thus the tides change approximately every 6 hours. The mean daily tidal range was approximately 0.6 m, while the minimum and maximum daily tidal ranges were 0.4 m and 1.0 m, during neap and spring tides, respectively.

Currents

The mean current speed at the three shallow (depth <10 m) sites was 0.21±0.12 m/s close to the surface and 0.05±0.03 m/s close to the seabed (fig. 5). The near-surface currents at MP4 and MP5 showed a strong, net offshore flow and were influenced more by wind speed and direction (fig. 5*C*,*D*) than those near the surface at the MP6 site (fig. 5*E*). The near-bottom currents at all three shallow (depth <10 m) sites also were influenced by the winds but were smaller in magnitude.

The mean current speed at the three offshore deep (depth ~20 m) sites ± one standard deviation was 0.33±0.17 m/s close to the surface and 0.21±0.12 m/s close to the seabed (fig. 6), approximately 50 percent greater than mean speeds close to the surface at the shallower sites and four times greater than those near to the bed at the shallower sites. Both the near surface and near bed currents at all the deep sites did not correlate well with wind speed or direction. It appears that bathymetry, tides, and the influence of larger-scale, open-ocean flow exert greater influence on the magnitude and direction of the currents than do the winds.

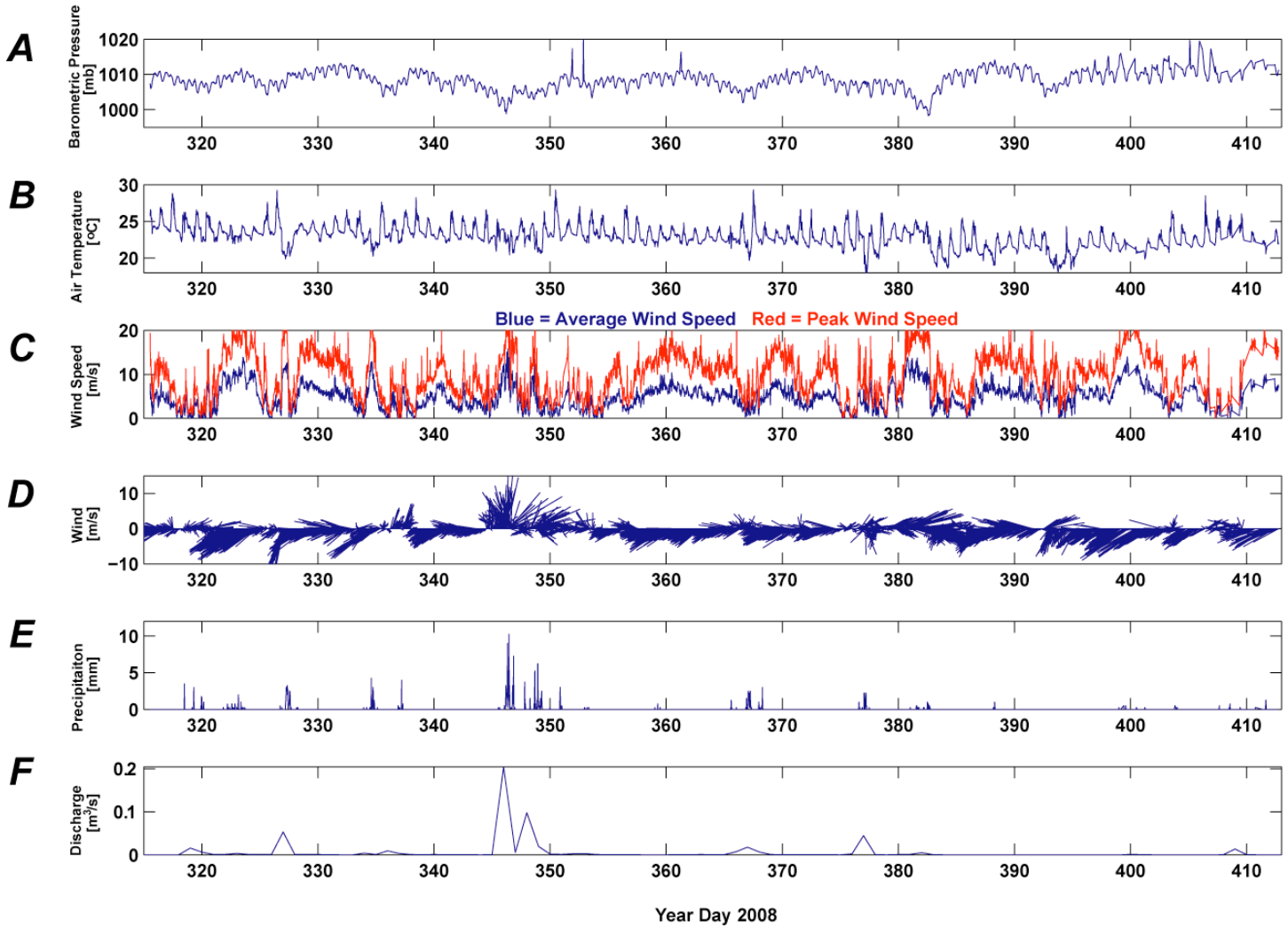

FIGURE 3. Meteorologic forcing data during the study period from the USGS weather station. *A,* Barometric pressure, in millibars. *B,* Air temperature, in degrees Celsius. *C,* Wind speed, in meters per second. *D,* Wind speed and direction, in meters per second from degrees true north. *E,* Rainfall, in millimeters. *F,* Stream discharge from the USGS H-1 # stream flow gauge, in meters cubed per second. The meterological data shows typical winter weather with periodic trade winds interspersed with strong winds from the south that typify Kona storms. Vectors show direction "going towards".

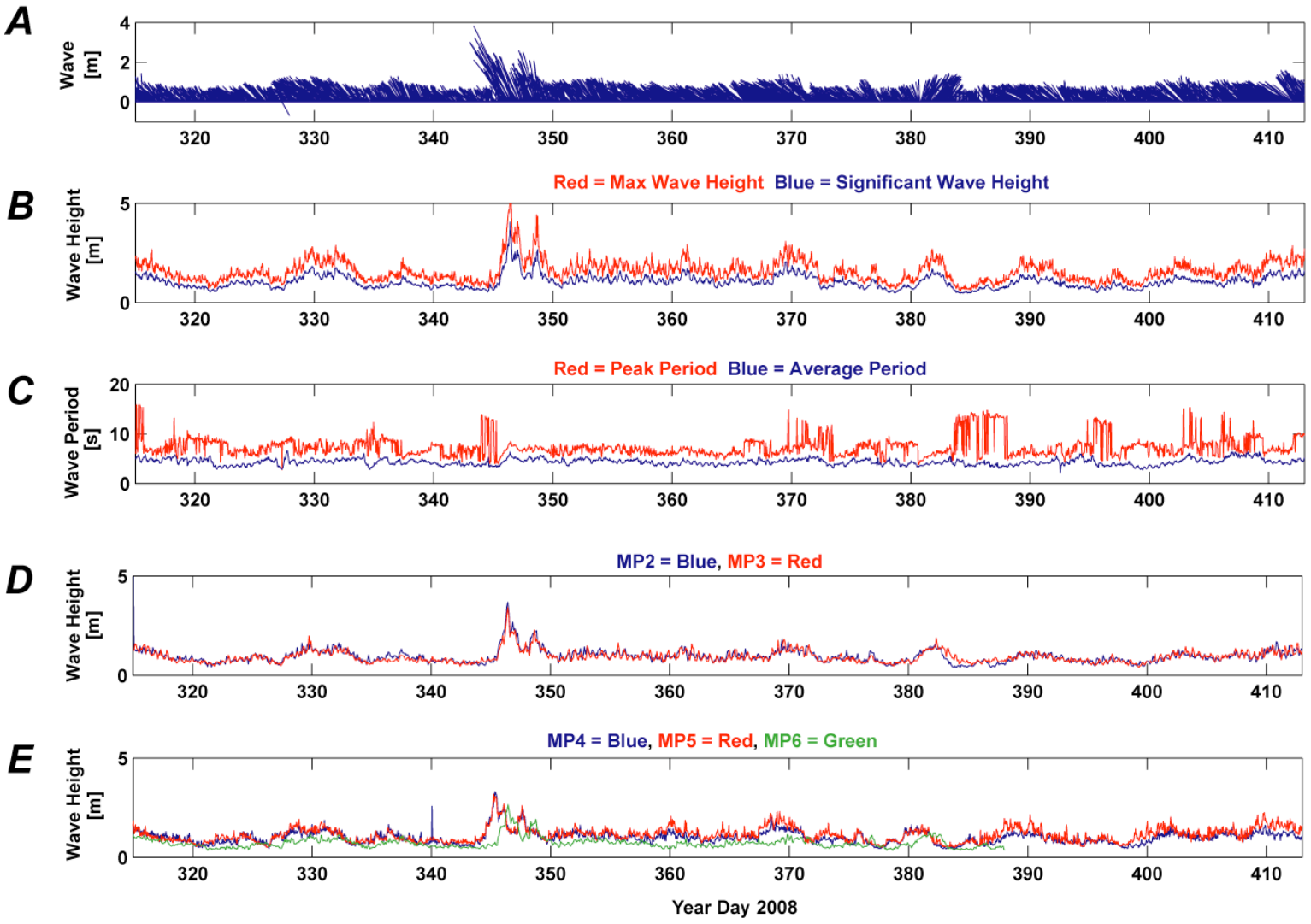

FIGURE 4. Oceanographic wave data for the entire study period. *A,* Wave direction. *B,* Average and peak wave height at the directional wave gauge (MP1). *C,* Average and peak wave period at site MP1. *D,* Average wave height at the other deeper sites (MP2 and MP3). *E,* Average wave height at the shallow sites (MP4 and MP5). The wave data shows transformation of waves as they move from deep to shallow water. Vectors show direction "going towards".

Temporal Variations Water Column Properties

The water-column properties that were measured by the deployed CTs and SLOBS included variations in temperature (ºC), salinity (PSU), and optical backscatter (NTU). The measurements were done to address the temporal variability in water-column properties over a range of forcing conditions.

Temperature

Water temperatures in the bay ranged from 23.65 to 26.36°C, with a mean temperature ± one standard deviation of 25.10±0.4°C (table 8). The inshore and offshore sites showed similar seasonal patterns in decreasing temperature during the deployment (fig. 7*A*,*C*). The diurnal temperature variations did not appear to be coherent across water depths. In some instances, the offshore sites showed greater day-to-day variations, while at other times the inshore sites showed greater diurnal variability. The non-coherence of water temperatures may be the result of tidally-driven interactions between deeper, cooler oceanic water and warmer nearshore waters.

Salinity

Salinity measurements in the bay ranged from 19.64 to 35.21 PSU, with a mean salinity ± one standard deviation of 34.83±0.31 PSU (table 9). The salinity measurements at the offshore and inshore sites display different trends and variability during the deployment (fig. 7*B*,*D*). Salinity at the offshore sites was fairly constant around 35 PSU but showed greater variability during times of heavy precipitation, suggesting that these sites may be influenced by freshwater discharge from streams or submarine groundwater discharge. The inshore sites also were relatively constant, with salinity values generally between 34 and 35 PSU, until the large precipitation from the December 11, 2008 (2008 Year Day 346), Kona storm. Salinity values at all the sites dropped significantly, with the largest decreases at the shallow MP6, MP5, and MP4 sites. The periods where Salinity values were low and variability was almost absent following the Kona storm at sites MP4 and MP5 are likely spurious data resulting from wave-driven sediment blocking the conductivity sensors.

Turbidity

Concurrent, reliable turbidity data were recorded for only 10 days (2008 YD 315-325) by all five of the SLOBS instruments; only the SLOBS at the MP4, MP5, and MP6 sites recorded data for the duration of the experiment (fig. 8). During the short time period with complete data coverage, the turbidity in the study area ranged between 0.00 and 31.94 NTU, with a mean turbidity ± one standard deviation of 0.87±1.09 NTU (table 10). The turbidity data for the longer time period (2008 YD 315-396) ranged between 0.16 and 136.57 NTU, with a mean turbidity ± one standard deviation of 2.68±4.35 NTU (table 10). Overall the turbidity in the bay is relatively low compared to previous measurements made elsewhere in the Main Hawaiian Islands except at the inshore sites MP4 and MP5, which consistently showed elevated turbidity values. The greatest turbidity values were measured during and shortly after the Kona storm from December 10-12, 2008 (2008 Year Day 345-347), that introduced large quantities of terrigenous sediment into the system. During this event, turbidity values exceeded 35 NTU for hours at the inshore (<10 m) sites, as discussed in greater detail in a later section of this report. Other periods of elevated turbidity occurred during periods when larger-than-normal waves impacted the bay (2008 Year Days 330, 370-390).

The State of Hawaii Department of Health's Administrative Rules, Title 11, Chapter 54, Water Quality Standards for "open ocean out to 600 foot depth", as defined on page 54-30 of that report (Department of Health, 2004), sets the maximum allowable wet season mean turbidity level at 0.50 NTU. The mean turbidity values for the period of study at sites MP4, MP5, and MP6 exceeded this threshold, and the mean turbidity value at the UH site (0.46 NTU) was barely below that threshold.

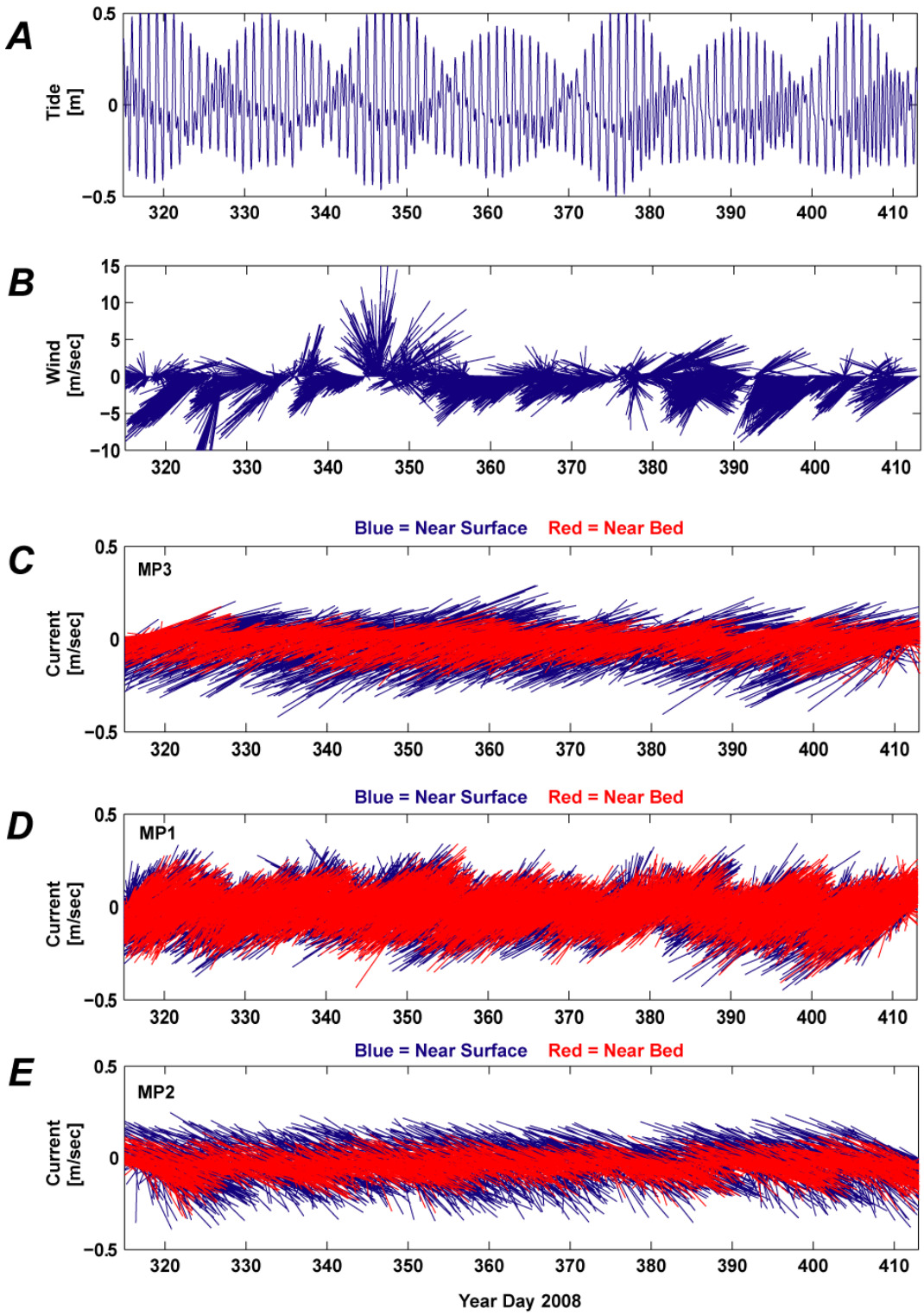

FIGURE 5. Current speed and direction and its relationship to wind at the shallow instrument sites. *A,* Tide, in meters. *B,* Wind speed and direction, in meters per second from degrees true north. *C,* Near surface (blue) and near bed (red) current speed and direction at site MP4, in meters per second from degrees true north. *D,* Near surface (blue) and near bed (red) current speed and direction at site MP5, in meters per second from degrees true north. *E,* Near surface (blue) and near bed (red) current speed and direction at site MP6, in meters per second from degrees true north. Vectors show direction "going towards".

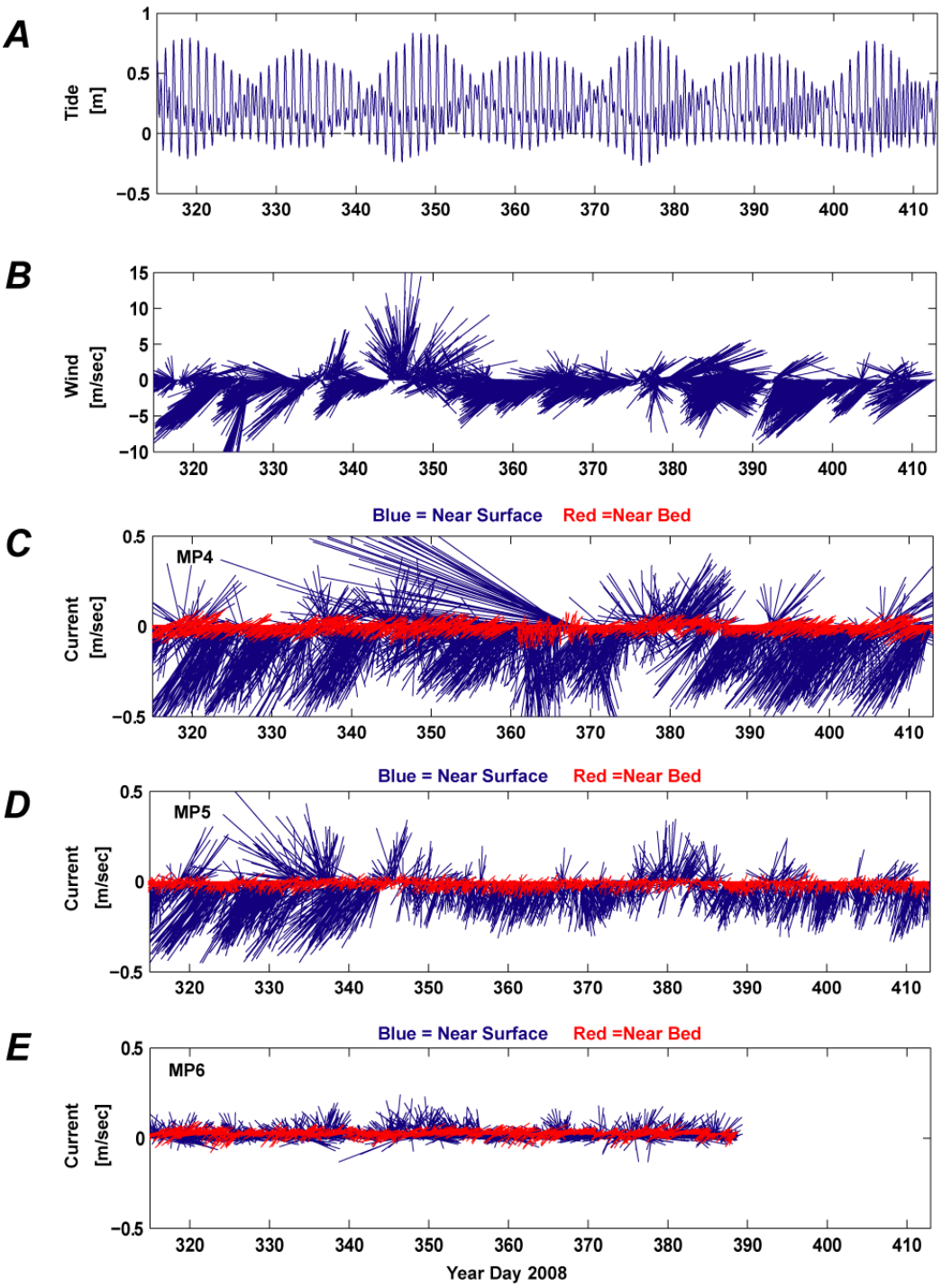

FIGURE 6. Current speed and direction and its relationship to wind at the deep instrument sites. *A,* Tide, in meters. *B,* Wind speed and direction, in meters per second from degrees true north. *C,* Near surface (blue) and near bed (red) current speed and direction at MP3, in meters per second from degrees true north. *D,* Near surface (blue) and near bed (red) current speed and direction at MP1, in meters per second from degrees true north. *E,* Near surface (blue) and near bed (red) current speed and direction at MP2, in meters per second from degrees true north. Vectors show direction "going towards".

The mean turbidity value at the MP5 site exceeded the maximum acceptable mean level by almost half an order of magnitude (table 5).

Spatial Variations in Water Column Properties

Spatial variations in water-column properties were measured in November 2008 and February 2009 at a greater number of locations within Maunalua Bay than the MPs using a vessel. The properties that were measured by the water column profiler included variations in temperature (ºC), salinity (PSU), turbidity (NTU), chl (mg/m^3), and DO (%) with depth. The surveys were done to address both along- and cross-shore variability in water-column properties in Maunalua Bay and to put the high temporal resolution but spatially-limited measurements made by the CTs and SLOBSs in the context of larger patterns throughout the bay. The greater density of sample locations near the coastline and in the Hawaii Kai Harbor channel was established to identify areas where terrestrial sediment or submarine groundwater discharge might be entering the bay. The profiles extended offshore to the 30 m isobath to examine the extent of mixing with oceanic waters.

In November 2008 (fig. 9*A*), depth-averaged water temperatures generally were lower and less variable closer to shore, except in the Hawaii Kai Harbor channel and off the paleostream channel at Kahala. During February 2009 (fig. 9*B*), however, the variability in water temperature was greatest close to shore, possibly due to cooler fluvial or submarine groundwater inputs. Overall, the water temperature throughout the bay was approximately 2°C cooler during the February 2009 survey than during the November 2008 survey. In November 2008 (fig. 10*A*), depth-averaged salinity values generally were higher and less variable closer to shore, except in the northeastern portion of the bay, including the Hawaii Kai Harbor channel. During February 2009 (fig. 10*B*), however, the variability in salinity was greatest close to shore in the western portion of the bay, possibly due to fluvial or submarine groundwater inputs. Overall, the salinity values throughout the bay were approximately 0.05 PSU greater during February 2009 than during November 2008.

In November 2008 (fig. 11*A*), depth-averaged turbidity values generally were greater and more variable closer to shore, especially in the Hawaii Kai Harbor channel. During February 2009 (fig. 11*B*), the turbidity were greatest in Hawaii Kai Harbor channel. Overall, the turbidity values throughout the bay were approximately 20 NTU lower during the February 2009 survey than during the November 2008 survey, suggesting the large inputs of sediment observed during the December 2008 Kona storm did not linger long in the bay under the environmental forcing conditions (winds and waves) that occurred between the December 2008 storm and the February 2009 survey. In both November 2008 (fig. 12*A*) and February 2009 (fig. 12*B*), depth-averaged chl values generally were greater in the northeastern portion of the bay, the Hawaii Kai Harbor channel, and offshore of Diamond Head in the southwestern portion of the bay. Overall, the chl values throughout the bay were approximately 0.3 mg/m^3 greater during the February 2009 than during the November 2008 survey, possibly due to the introduction of nutrients either through fluvial or submarine groundwater sources following the heavy rainfall that occurred during the December 2008 Kona storm. The spatial patterns of DO in Maunalua Bay during both the November 2008 (fig. 13*A*) and February 2009 (fig. 13*B*) were not consistent except for lower values in the Hawaii Kai Harbor channel.

Sediment Composition and Grain Size

The grain size of the seabed at the instrument sites primarily was sand (mean for all sites = 95.0%) with a small amount of gravel (mean = 4.6%; fig 14*A*). The largest grain sizes of the seabed were found at MP3, approximately 80% sand and 20% gravel, likely a result of the strong currents and large waves winnowing out any finer-grained material delivered to the area (tables 11-12). The grain size of the sediment collected in the traps shows a very different distribution than the grain size of the

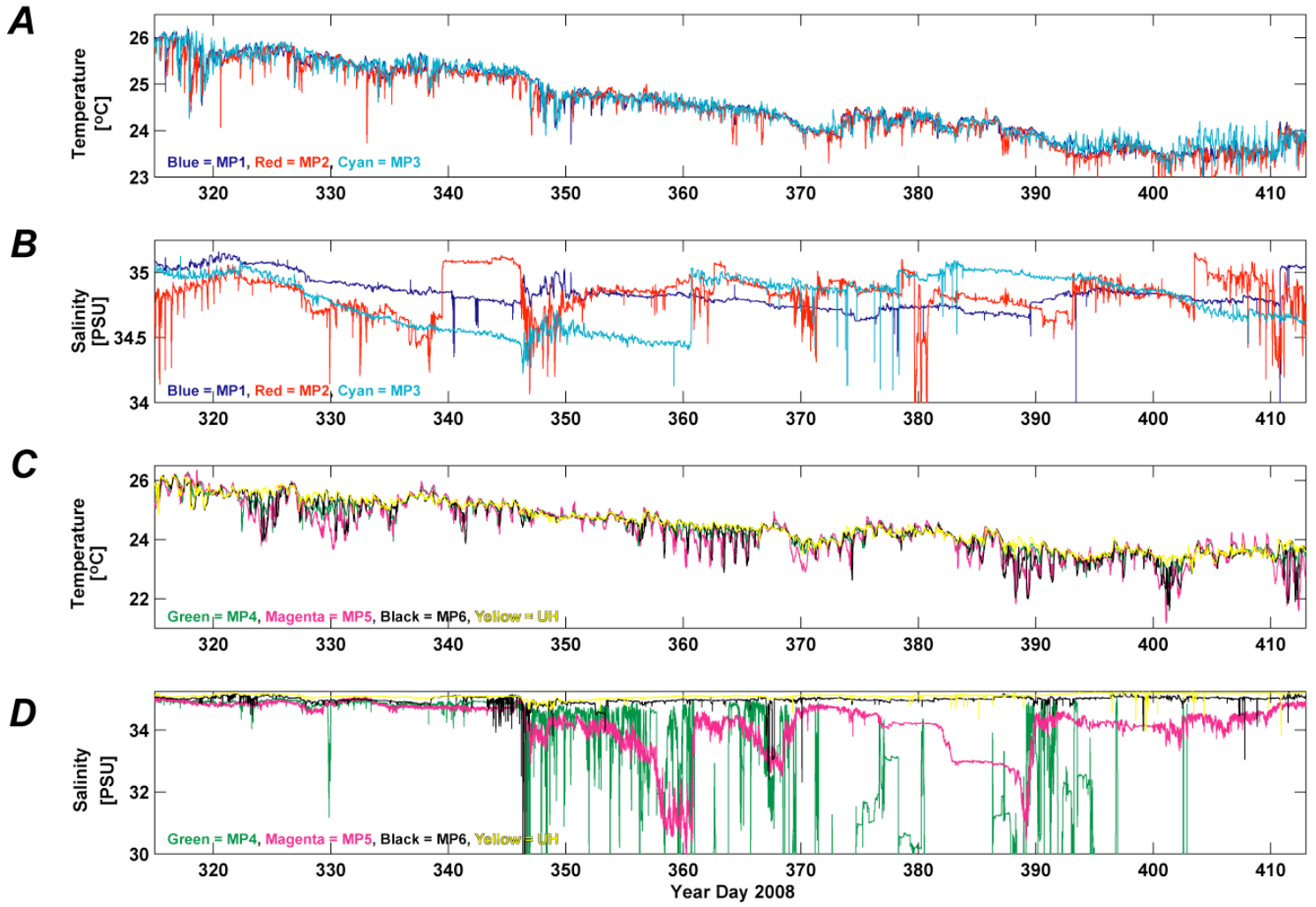

FIGURE 7. Variability in temperature and salinity variability at the main study sites. *A,* Temperature at the deep sites, in degrees Celsius. *B,* Salinity at the deep sites, in Practical Salinity Units. *C,* Temperature at the shallow sites, in degrees Celsius. *D,* Salinity at the shallow sites, in Practical Salinity Units. The temperature data shows the seasonal trend of cooling through the winter months at both the deep and shallow sites, with greater daily fluctuations at the shallow sites due to daily insolation. The salinity data is relatively constant at the shallow sites up until the large precipitation event December 11, 2008 (2008 Year Day 346).

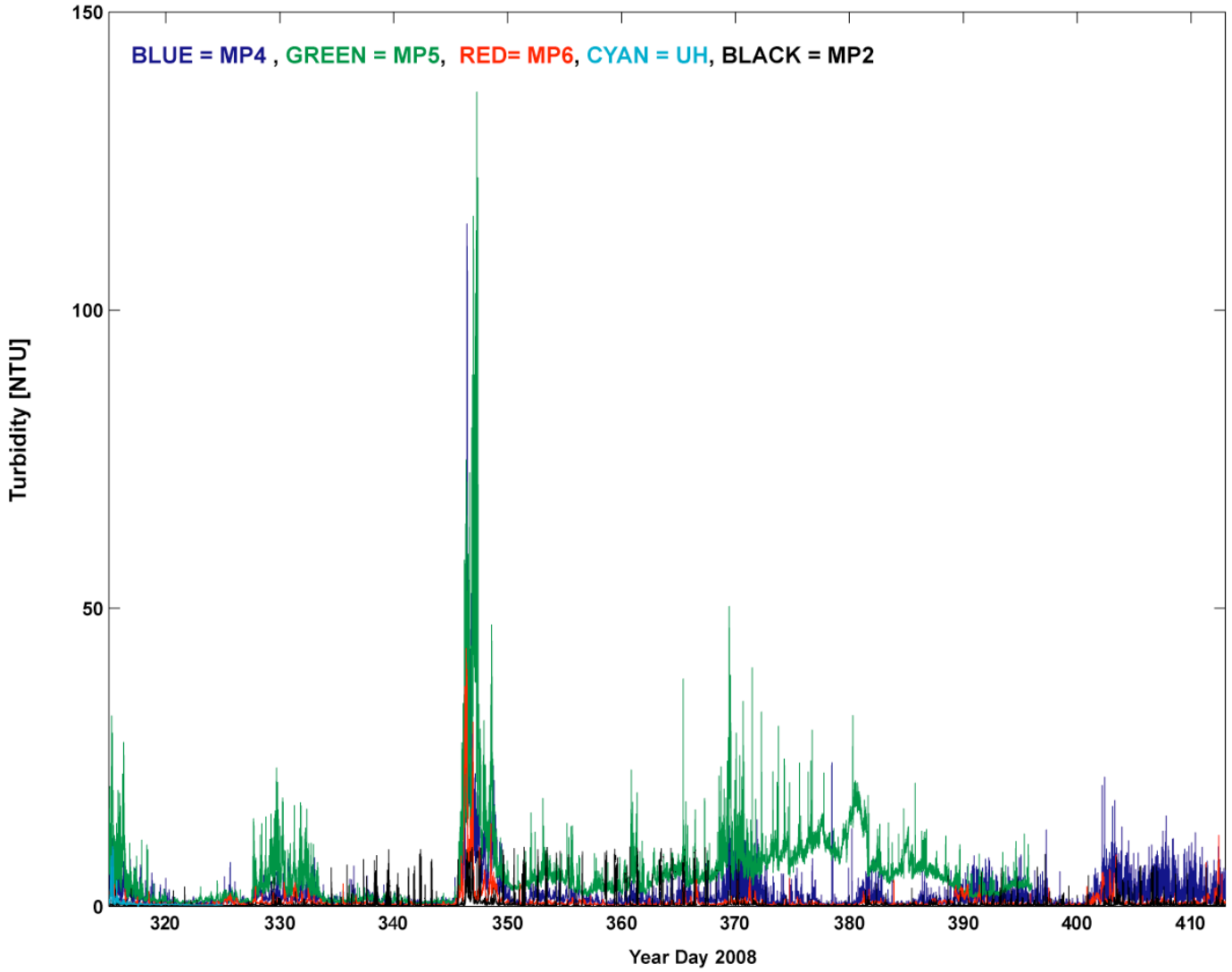

FIGURE 8. Turbidity at the instrument sites, in Nephelometric Turbidity Units. The shallow sites, specifically site MP5, showed high turbidity values during the Kona storm event of December 11, 2008 (2008 Year Day 346), as well as during other turbidity events due to lesser precipitation or large wave events.

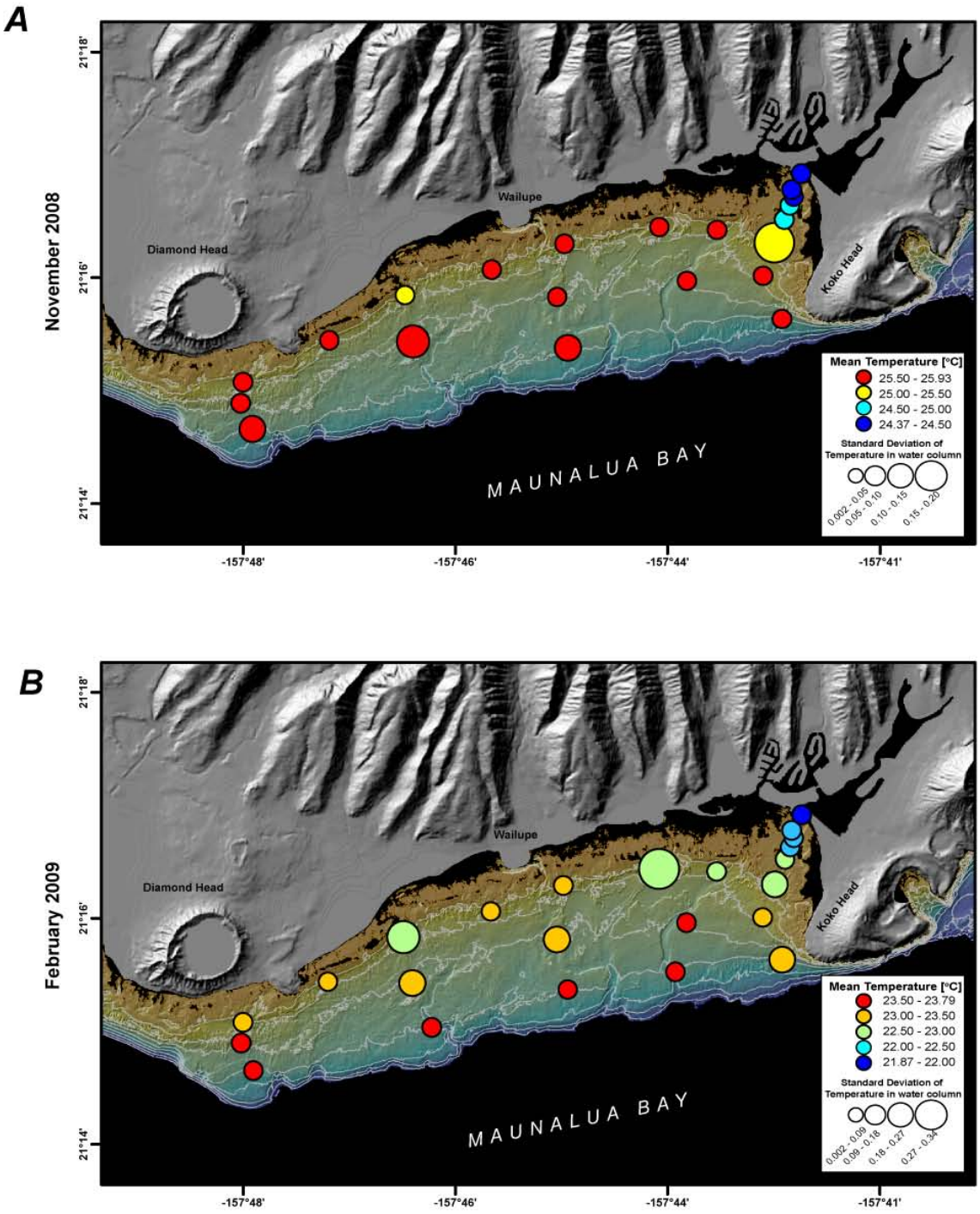

FIGURE 9. Spatial variability in temperature, in degrees Celsius, from the Water Column Profiler (WCP) surveys. *A,* Data from the November 2008 survey. *B,* Data from the February 2009 survey. In November 2008, depth-averaged water temperatures generally were lower and less variable closer to shore, except in the Hawaii Kai Harbor channel and off the paleostream channel at Kahala. During February 2009, however, the variability in water temperature was greatest close to shore, possibly due to cooler fluvial or submarine groundwater inputs. Overall, the water temperature throughout the bay was approximately 2°C cooler during the February 2009 survey than during the November 2008 survey.

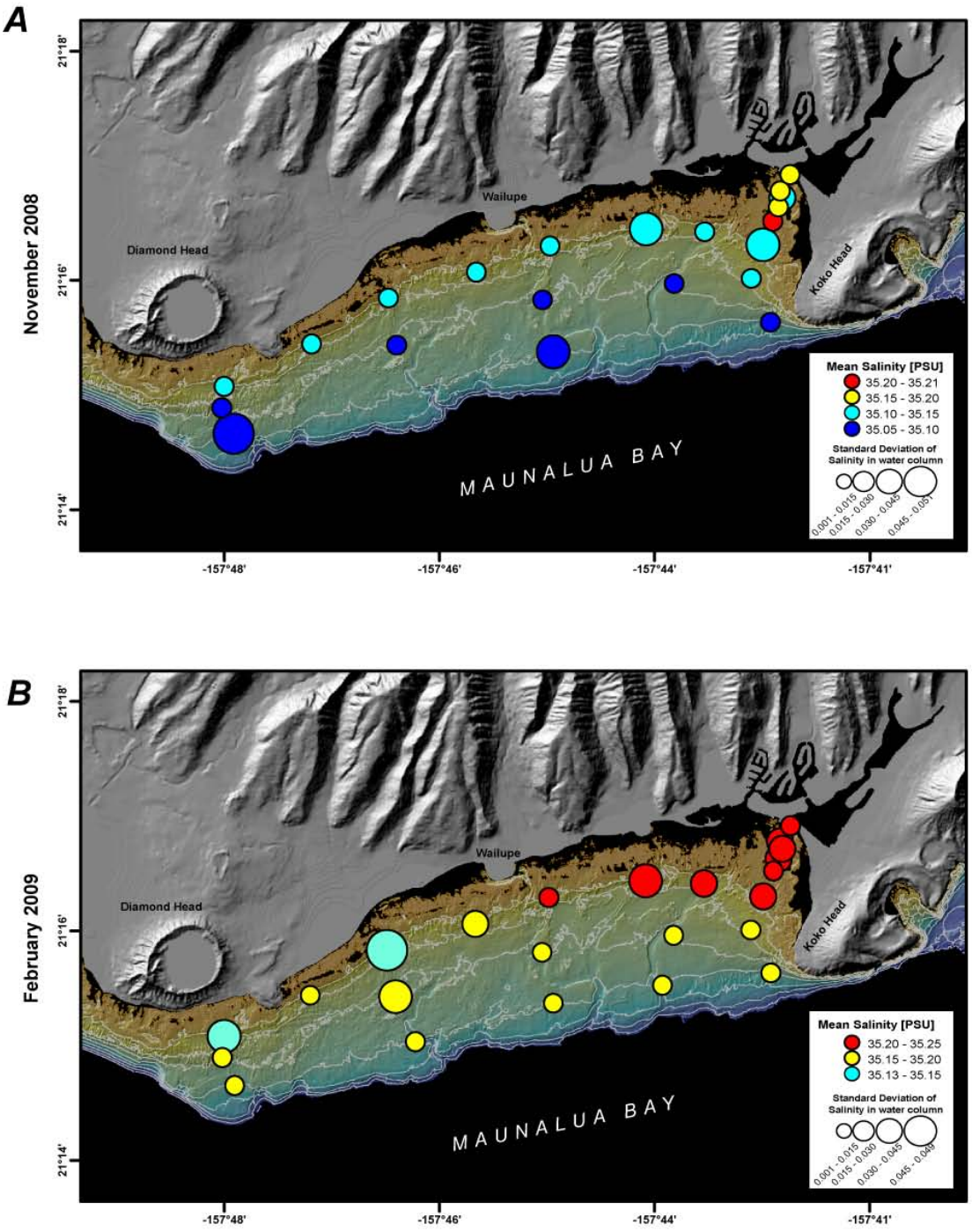

FIGURE 10. Spatial variability in salinity, in Practical Salinity Units, from the Water Column Profiler (WCP) surveys. *A,* Data from the November 2008 survey. *B,* Data from the February 2009 survey. In November 2008, depth-averaged salinity values generally were higher and less variable closer to shore, except in the northeastern portion of the bay, including the Hawaii Kai Harbor channel. During February 2009, however, the variability in salinity was greatest close to shore in the western portion of the bay, possibly due to fluvial or submarine groundwater inputs. Overall, the salinity values throughout the bay were approximately 0.05 PSU higher during February 2009 than during November 2008.

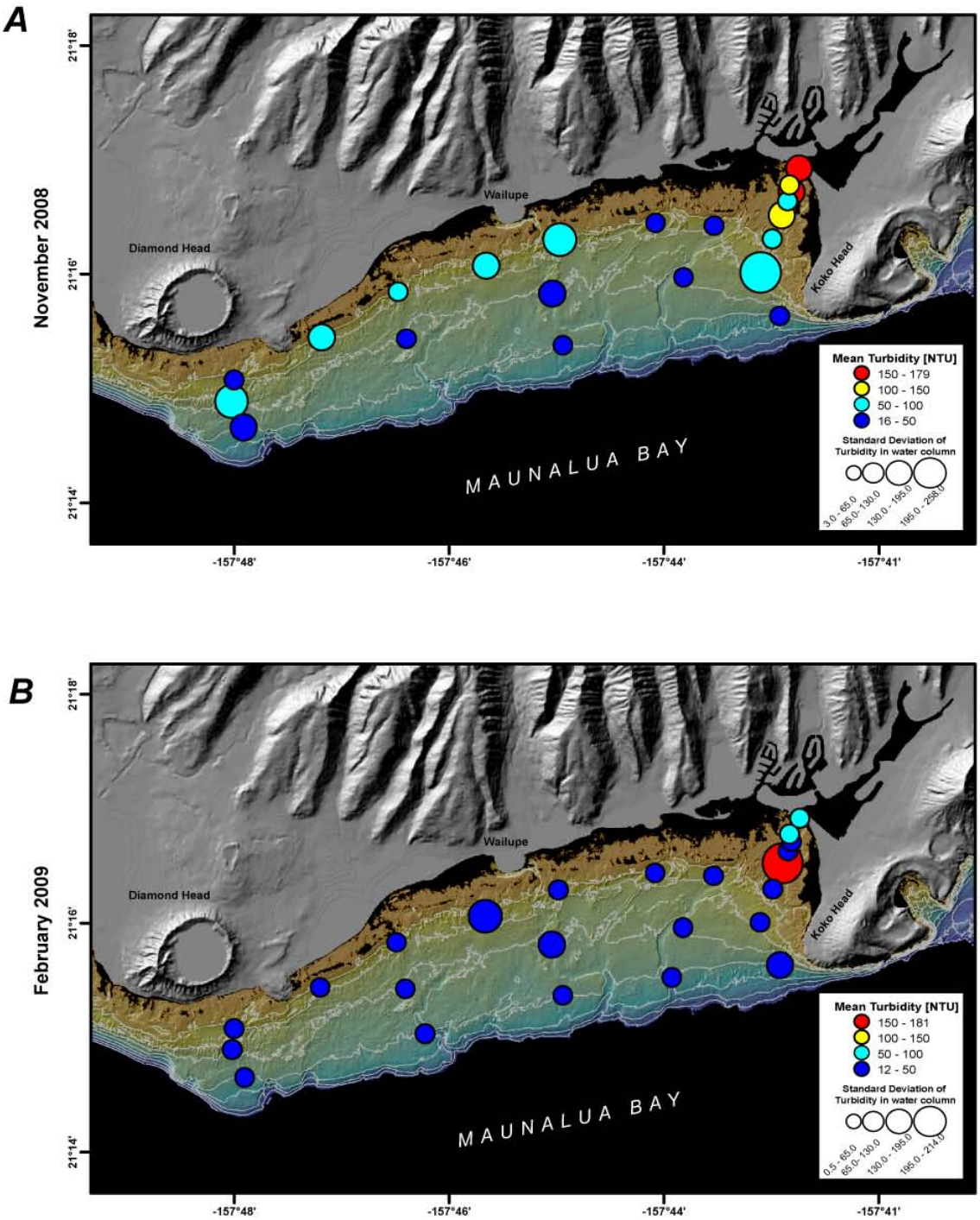

FIGURE 11. Spatial variability in turbidity, in Nephelometric Turbidity Units, from the Water Column Profiler (WCP) surveys. *A,* Data from the November 2008 survey. *B,* Data from the February 2009. In November 2008, depth-averaged turbidity values generally were higher and more variable closer to shore, especially in the Hawaii Kai Harbor channel. During February 2009, the turbidity still was highest in Hawaii Kai Harbor channel. Overall, the turbidity throughout the bay was approximately 20 NTU lower during the February 2009 survey than during the November 2008 survey, suggesting the large inputs of sediment observed during the December 2008 Kona storm did not linger long in the bay.

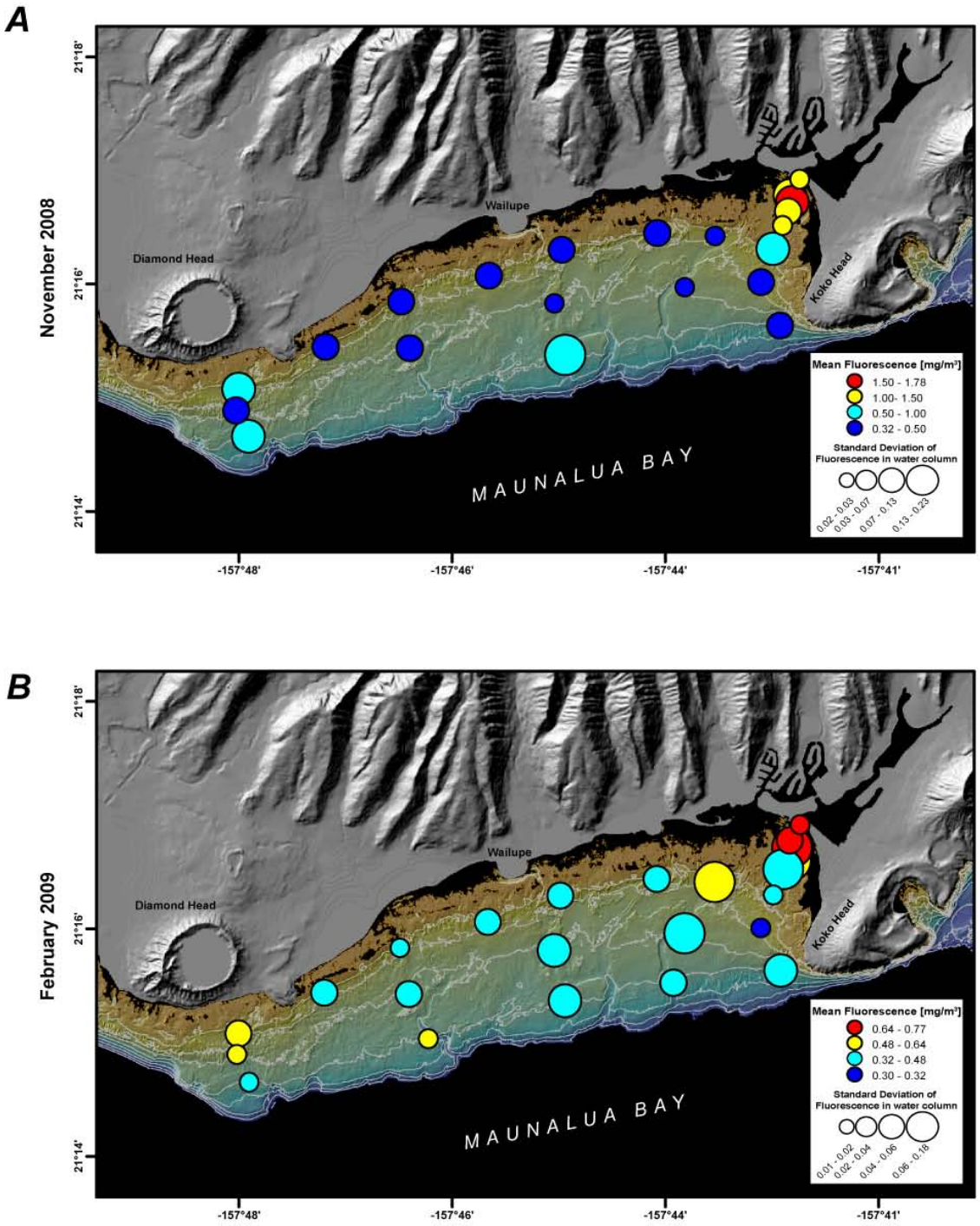

FIGURE 12. Spatial variability in fluorescence, in milligrams per cubic meter, from the Water Column Profiler (WCP) surveys. *A,* Data from the November 2008 survey. *B,* Data from the February 2009. In both November 2008 and February 2009, the depth-averaged fluorescence generally was higher in the northeastern portion of the bay, the Hawaii Kai Harbor channel, and offshore of Diamond Head in the southwestern portion of the bay. Overall, the fluorescence throughout the bay was approximately 0.3 mg/m^3 higher during the February 2009 survey than during the November 2008 survey, possibly due to the introduction of nutrients through either fluvial or submarine groundwater sources.

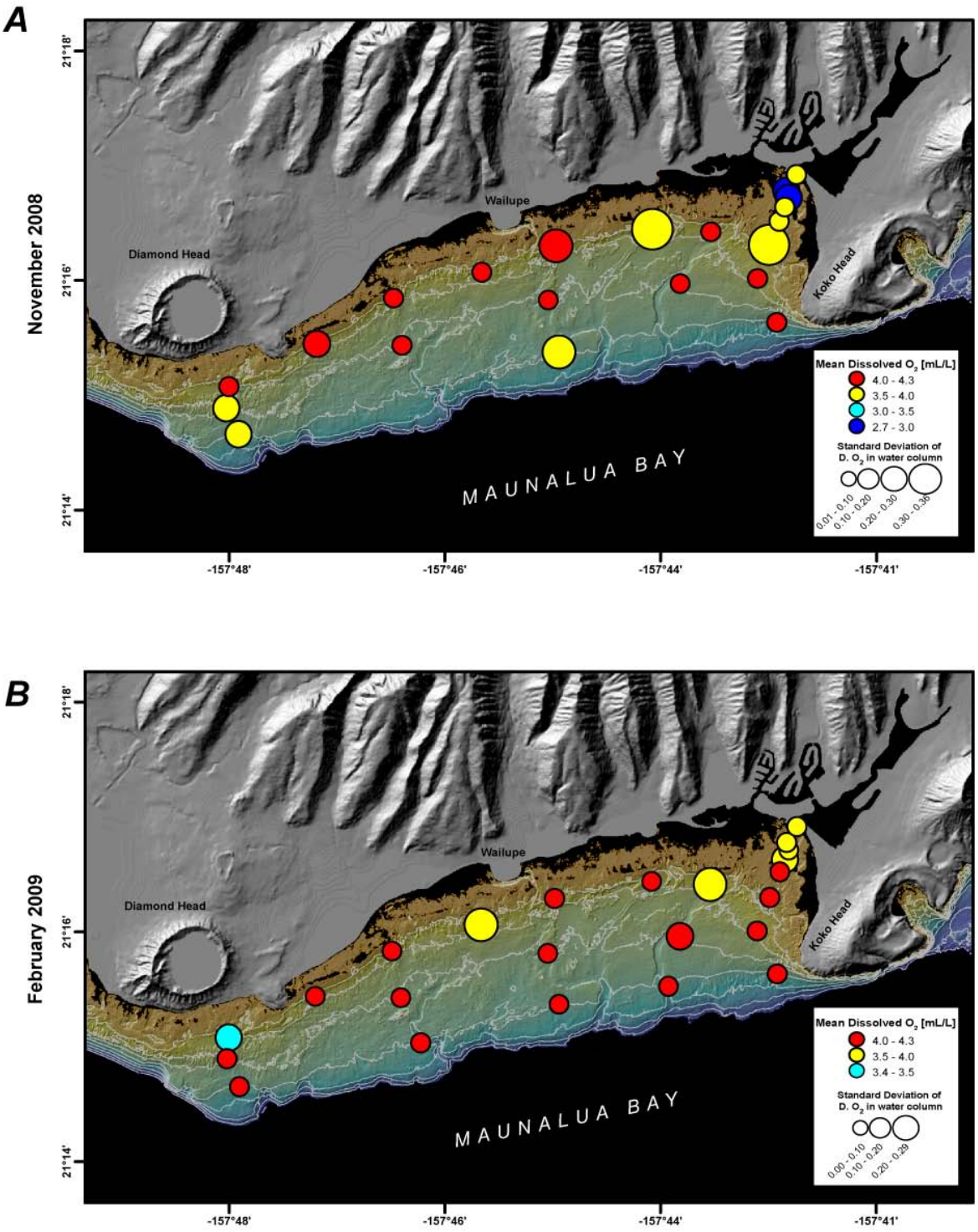

FIGURE 13. Spatial variability in dissolved oxygen, in milliliters per liter, from the Water-Column Profiler (WCP) surveys. *A,* Data from the November 2008 survey. *B,* Data from the February 2009. The spatial patterns of dissolved oxygen in Maunalua Bay during both the November 2008 and February 2009 were not consistent except for lower values in the Hawaii Kai Harbor channel.

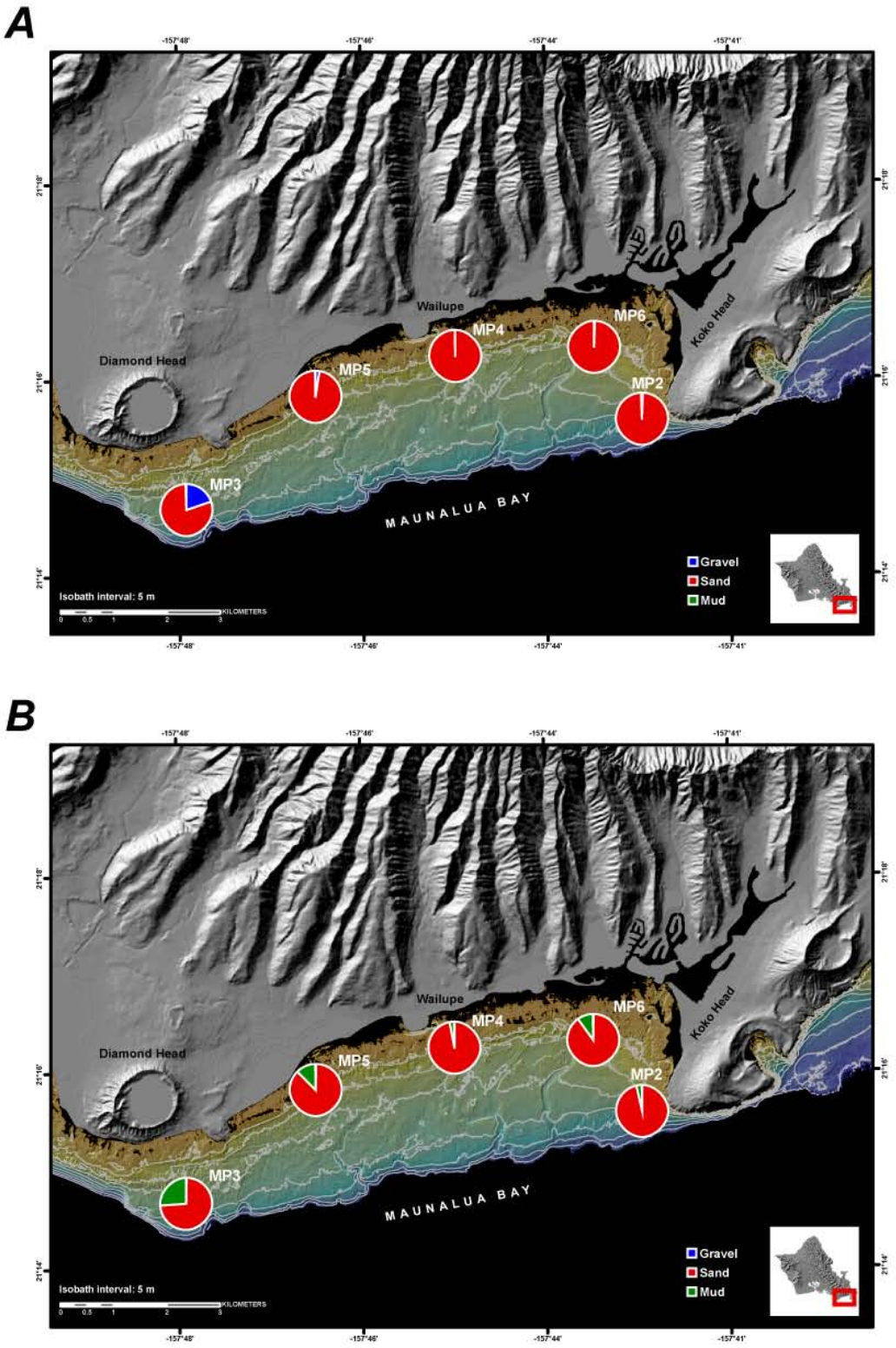

FIGURE 14. Grain size of sediment at the main study sites, in percentage by class. *A,* On the seabed. *B,* Collected in sediment traps. The seabed sediment at all sites is coarser than the material collected in the co-located sediment traps.

seabed samples. The grain size in the traps primarily was sand (mean = 88.7%), with a larger component of mud than in the seabed samples (mean = 11.1% versus 0.4% for seabed samples; fig 14*B*). This demonstrates that there was fine-grained muddy sediment transported through the system but, given the wave energy and current speeds, it was not able to settle and remain on the seabed for long durations. This difference in grain size between the seabed and what accumulates in sediment traps is not uncommon. Finer-grained, lighter particles can be resuspended more easily and carried higher up into the water column and thus to the height of the trap's opening, than can coarser particles. Once these fine-grained particles settle into the trap, they cannot be resuspended and advected away as could the same-sized material on the adjacent seabed (e.g., Bothner et al., 2006).

The composition of the sediment on the seabed primarily was bioclastic reef-derived calcium carbonate (mean = 94.6%) at all of the instrument sites (fig. 15*A*; table 13). All sites had a minor (mean = 11.4%) component of total inorganic carbon and an even smaller percentage (mean = 5.4%) of terrigenous material. The composition of sediment collected by the sediment traps at all of the instrument sites was also primarily reef-derived calcium carbonate (mean = 86.2%), but all traps had a larger component of terrigenous sediment (mean = 13.8%) than the seabed samples (fig. 15*B*). Sediment traps often are better indicators of the type of sediment being transported through the system than indicators of net deposition on the seabed (e.g., Bothner et al., 2006). Sites MP3, MP5, and MP6 had the largest components of terrigenous sediment, indicating these areas may be where the terrigenous sediment is introduced into the bay. More than twice as much terrigenous sediment was collected in the traps than was observed on the seabed, suggesting that very little terrigenous sediment was deposited on the bay's seabed, and that it primarily was advected through the system because of the predominantly small grain size. Overall, the trap collection rates at the shallow (<10 m depth) sites exceeded 70 $mg/cm^2/day$ and were greater off the northwestern portion of the bay's (off Kahala) reef flats than off the northeastern portion of the bay's reef flats (Paiko Lagoon; table 11). These high trap accumulation rates (>70 $mg/cm^2/day$) potentially can result in mortality of adult corals (Phillip and Fabricius, 2003); however, as shown by the geochemistry, much of this material was carbonate in origin and thus likely due to resuspension of the surrounding seabed material rather than to the net influx of terrestrial sediment.

Discussion

Distribution of Forcing Conditions

The deployment in Maunalua Bay took place during the months of November – February, at the transition from steady, dry, trade-wind season to the winter, which is characterized by rain and inconsistent trade winds (fig. 3). During the deployment four dominant conditions were observed and quantified: trade wind, variable winds, Kona storm, and south swell (fig. 16).

Trade wind conditions were defined as wind speeds greater than 4 m/s and wind directions between 45° and 135°T. This condition occurred during approximately 50% of the deployment period, which is consistent with analyses of observations made elsewhere in the Hawaiian Islands (Presto et al, 2006). The second most prevalent condition (40%) of the deployment period was variable/low winds, which are characterized by wind speeds less than 4 m/s and waves smaller than 1 m. During these times tidal currents and/or large-scale oceanographic forcing conditions (for example, eddies) are the primary mechanisms driving nearshore circulation. South swell, the third most prevalent condition (7% of the deployment), was characterized by waves from directions greater than 170°T, with significant wave heights greater than 1 m. These swells often are generated far away from the Hawaiian Islands and are not often associated with locally strong winds or precipitation. The least prevalent condition (3% of the

deployment period) was Kona storms. Kona storms are episodic, locally generated low-pressure systems that often move from the south to north during the winter months and are associated with high rainfall and strong south winds. Kona storms were defined as those periods with wind speeds greater than 4 m/s and wind directions between 135 and 225°T.

Spatial and Temporal Variability in Circulation Patterns and Water Column Properties

Tides, trade winds, and waves occurred on different time scales during the experiment and contributed to the overall circulation in the bay and the resulting flux of fresh water and sediment. The resulting circulation patterns are described below for each of the oceanographic conditions and their implications for the delivery of sediment to different portions of the bay.

Tides

Tides drive most of the daily variability in current speed and direction in Maunalua Bay. During flood (rising) tide, the near-surface currents are predominantly to the west and offshore at most of the instrument sites (fig. 17*A*). The near-surface currents at the MP2 site are to the west and onshore, while at site MP3 the near-surface currents are to the east and offshore, resulting in a counter-clockwise circulation in the bay. During the ebb (falling) tide, the near-surface currents are to the east and slightly onshore at most of the instrument sites (fig. 17*B*). The near-surface currents are to the east and offshore at MP2 and to the west and onshore at MP3. During the ebb tide, the near-surface currents create a clockwise circulation cell in the bay. The near-surface currents during the flood tide appear to be slightly stronger than during the ebb tide at all instrument sites. The principal axes of flow are oriented primarily along the bathymetry. The near-bed tidal currents mimic the near-surface currents in direction, but are smaller in magnitude.

Winds

Near-surface currents during trade-wind conditions show a circulation pattern influenced by wind speed and direction. The near-surface currents at all of the sites are affected by the strong, consistent, easterly trade winds (fig 18*A*). Currents are oriented primarily offshore and slightly to the west, suggesting that the bay is flushed of water under this kind of forcing. An exception to this general offshore flow pattern was observed at site MP6, where the currents flowed into the wind, toward the east, suggesting that there must be some sort of recirculation feature bringing water onshore and up into the northeast corner of the bay that was not captured by one of the instruments due to the large distance between sites. Near-bed currents (fig. 18*B*) also mimic the direction of the near-surface currents, but are smaller in magnitude. Near-bed turbidity during trade-wind conditions was minimal (<10 NTU) at all of the instrument sites, suggesting that very little seabed sediment was resuspended and transported by trade-wind forcing.

Waves

The deployment period coincided with periods of large waves from the south that typically are associated with summer conditions, thus providing information on circulation during those periods. Near-surface currents during large wave events are shown in figure 19a. At most of the sites in the bay, the near-surface current direction was primarily offshore, and at site MP1 and MP6 the currents were alongshore. The diversion of water to the west at sites MP1 and MP4 and to the east at sites MP 2 and MP6 suggests that there must be a recirculation feature bringing water onshore and up into the northeast corner of the bay that was not captured by one of the instrument due to the large distance between the sites. Near-bed currents were similar to the near-surface currents in direction but were much smaller in magnitude (fig. 19b). The offshore direction of currents during large wave events may be a mechanism

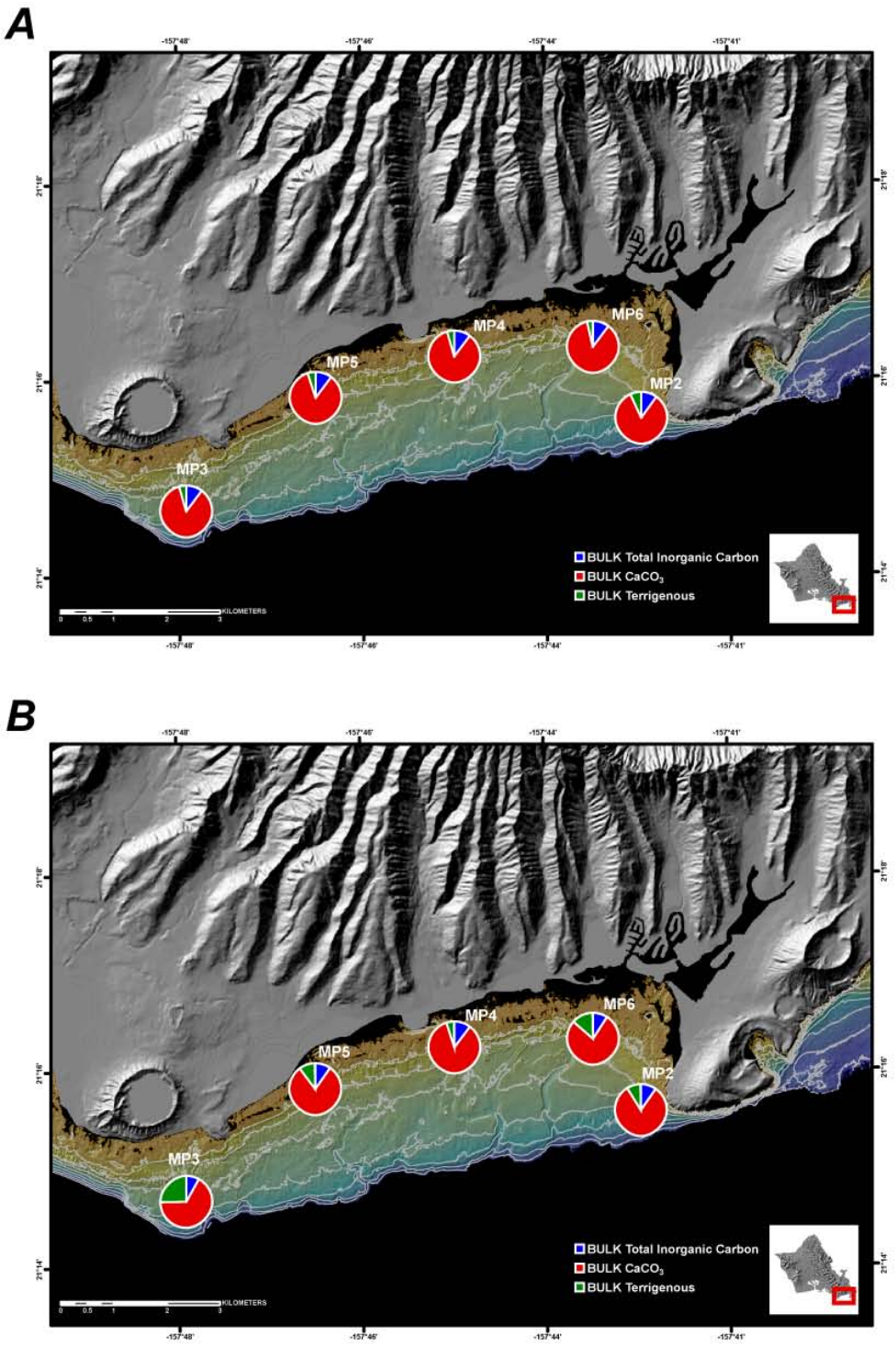

FIGURE 15. Composition of sediment at the main study sites, in percent. *A,* On the seabed. *B,* Collected in sediment traps. The sediment on the seabed and collected in the co-located traps predominantly is carbonate and likely is derived from the reefs in the bay. Approximately twice as much material collected in the sediment traps was terrestrial in orgin than was found on the seabed, suggesting that terrestrial sediment is fluxing through the system but is not stable on the seabed under the oceanographic conditions that occured during the study.

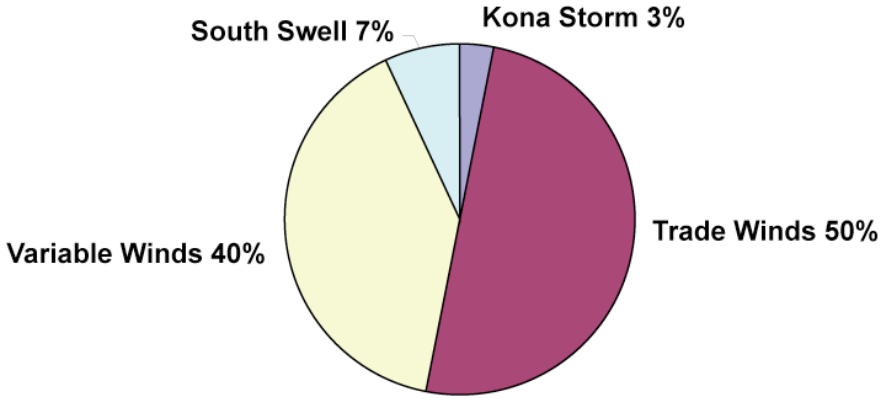

FIGURE 16. Pie chart showing the relative distribution of forcing conditions observed in Maunalua Bay during the November 2008-February 2009 study period. Approximately 50 percent of the deployment period was characterized by trade-wind forcing (wind speeds >4 m/s and wind directions between 45°T and 135°T) and variable/low winds conditions (wind speeds <4 m/s and waves <1 m) occurred 40 percent of the time. South swell forcing (waves from directions >170°T with significant wave heights >1 m) characterized 7 percent of the deployment and Kona storm conditions (wind speeds >4 m/s and wind directions between 135°T and 225°T) occurred 3 percent of the time.

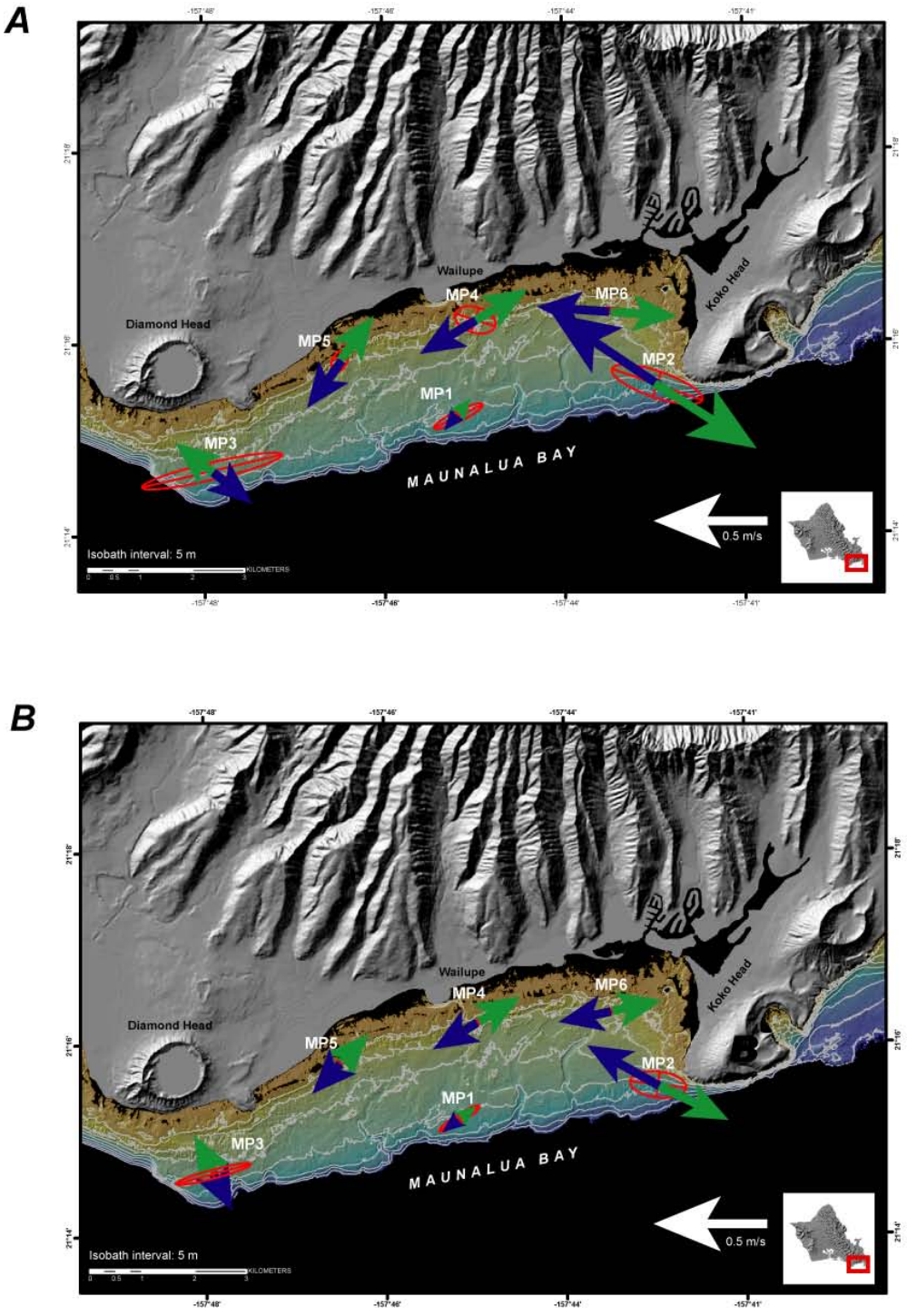

FIGURE 17. Principal axis ellipses and mean current speeds and directions, in meters per second from degrees true north, during conditions dominated by tidal flow at the main study sites. *A,* Close to the surface. *B,* Close to the seabed. The mean orientation and magnitude of flow during ebb (falling) and flood (rising) tides are shown in green and blue, respectively. The tidal ellipses (red) were oriented primarily parallel to the isobaths, predominantly in an east-west direction. In general, the tidal currents flooded (rose) to the west and slightly offshore and ebbed (fell) to the east and onshore.

for transporting sediment out of the bay during the summer months after sediment is delivered to the bay from winter precipitation and stream discharge.

Near-bed turbidity during wave conditions out of the south was greater (20-50 NTU) than during trade-wind conditions at all of the instrument sites, suggesting that the shear stresses generated from the large waves were sufficient to have caused the resuspension of seabed sediment. When large waves coincided or followed sediment and freshwater input from local streams, the largest turbidity values (>100 NTU) of the experiment were observed at the inshore sites (MP4 and MP5). The quick return of turbidity to pre-event levels indicates that the sediment in suspension predominantly was sand, as indicated by the sediment trap and seabed sample data.

Kona Storm

A large Kona storm brought strong south winds, large waves, and more than 95 mm of rainfall to the Maunalua Bay region during a 3-day period from December 11-13, 2008 (2008 Year Day 346-348). The large amount of rainfall during the short period of time resulted in large amounts of terrestrial sediment being transported into the bay. Near-surface currents in the bay show a pattern of alongshore flow toward the middle of the bay and offshore flow to the east (fig. 20*A*). Near-bed currents show alongshore flow to the east and slightly offshore at the deep sites and variable directions at the inshore sites (fig. 20*B*).

A sequence of photos from the TIS shows the progression of the storm, with initially strong onshore (southerly) winds (fig. 21*A*) followed by large waves and heavy precipitation (fig. 21*B*). The waves are shown breaking in the outer part of the bay, indicating their large size (waves break in water depths relative to their height, so larger waves break in deeper water); these large waves appear to have generated near-bed shear stresses sufficient to resuspend carbonate material on the seabed as inferred from the anomalous light color of the water offshore. Just before noon on December 11 (2008 Year Day 346), the terrestrial sediment-laden plume exited the lagoon east of Hawaii Kai and entered the bay off the western slope of Koko Head (fig. 21*C*). By mid-afternoon, the surface plume had been advected west past the Paiko Lagoon along the fore reef (fig. 21*D*).

An increase in turbidity due to either wave resuspension of seabed material or the injection of terrestrial material into the bay was recorded by all of the operational SLOBS in the bay. The turbidity levels increased first at site MP5, followed by site MP4, site MP6, and site MP2. The largest increase and duration in turbidity was observed at site MP5, with values exceeding 120 NTU (fig. 22) and greater than 35 NTU for more than 1,065 min (~17.8 hours); the turbidity values exceeded 35 NTU for 50 min at site MP6 and 310 min (~5.2 hours) at site MP4. The turbidity at MP6 also was imaged by the CIS (fig. 23). Before the storm, the coral head and calibration block can be seen clearly in the imagery (fig. 23*A*,*B*). By noon, the turbidity had exceeded 35 NTU, resulting in a complete "brown-out" at the MP6 site (fig. 23*C*), resulting in no sunlight reaching the seabed and thus a complete shut-down of photosynthesis. The imagery from the day following the storm on December 13, 2008 (2008 YD 348) showed much lighter (whiter) material in suspension (fig. 23*D*), suggesting the sediment imaged was carbonate seabed material resuspended by waves, and that the terrestrial sediment imaged during the storm was no longer the dominant material in the water column and had been advected away. This rapid advection of the material away from site MP6 also is supported by the SLOBS data, which showed greater (>40 NTU) turbidity values during the storm, but only for a relatively short duration (50 min; fig. 22).

The salinity and temperature values at the offshore and inshore sites during the Kona storm show a significant freshwater signal in the bay (fig. 24). The temperature signal at the offshore sites showed a minor decrease during the period of heavy precipitation. The salinity also showed a slight decrease at sites MP2 and MP3 and little change at site MP1, indicating a significant freshwater signal was not

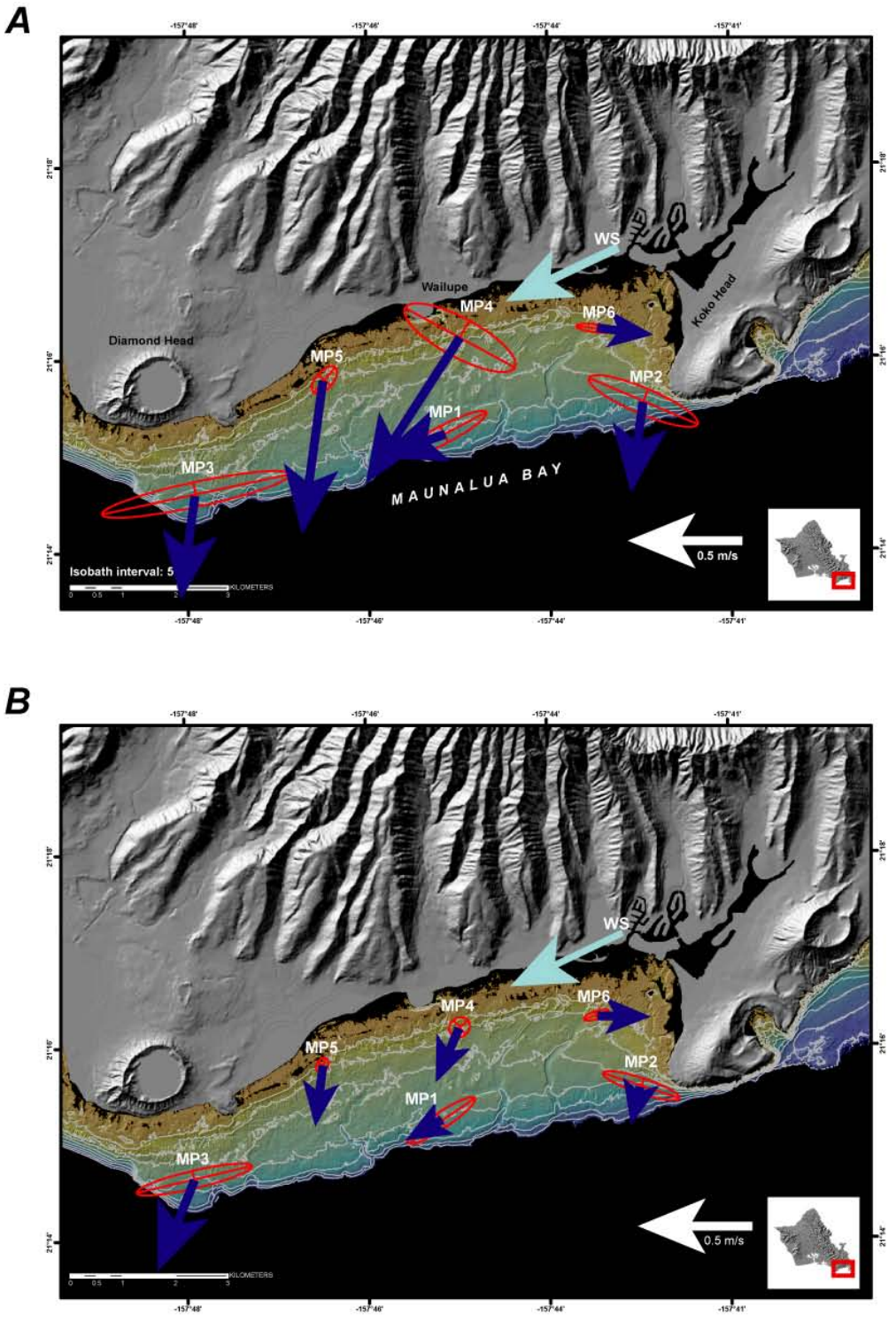

FIGURE 18. Principal axis ellipses and mean current speeds and directions, in meters per second from degrees true north, during strong trade-wind conditions at the main study sites. *A,* Close to the surface. *B,* Close to the seabed. The principal axis ellipses were oriented primarily along the isobaths and the near surface current directions were predominantly to the west, approximately down-wind.

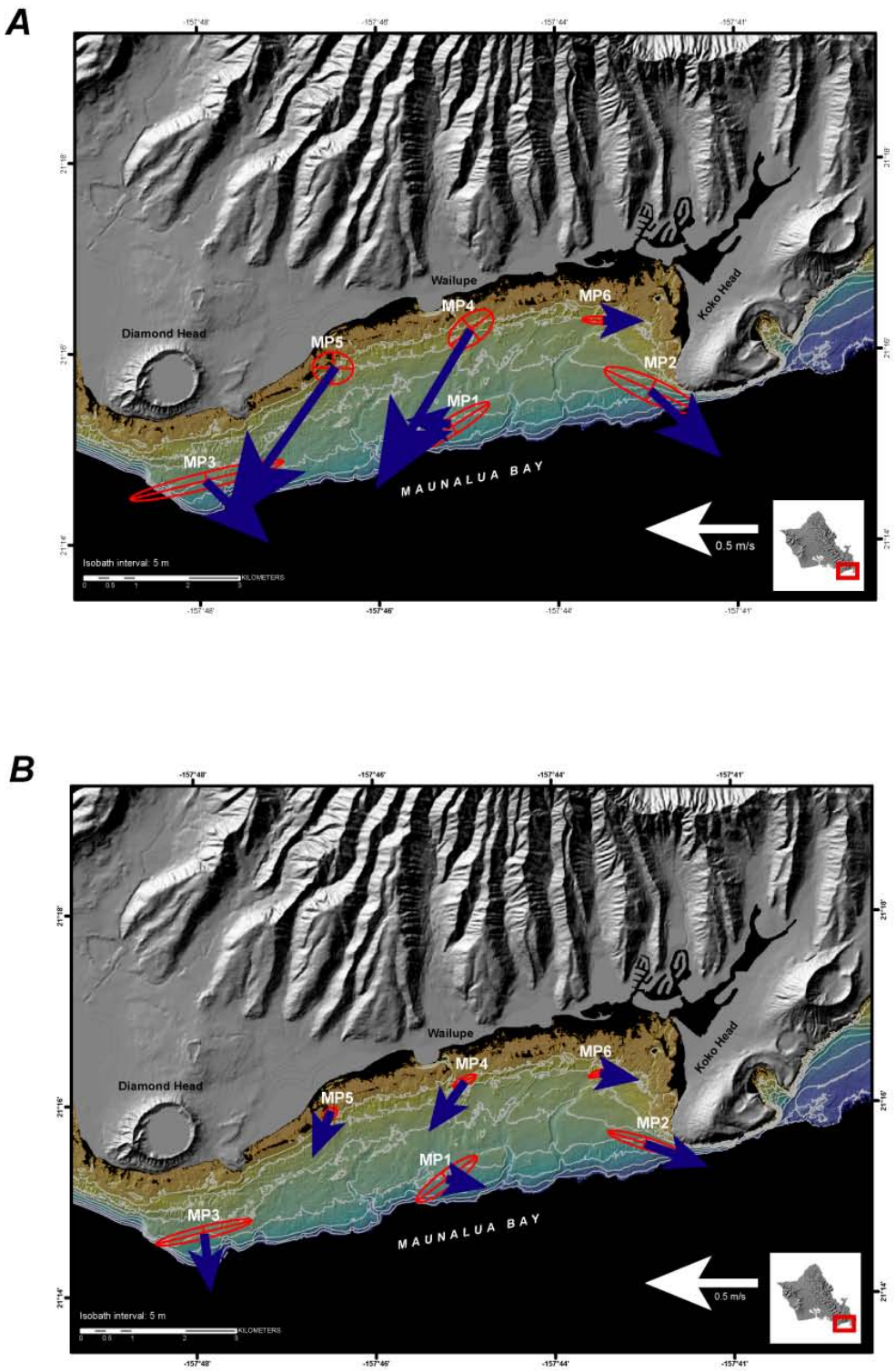

FIGURE 19. Principal axis ellipses and mean current speeds and directions, in meters per second from degrees true north, during large-wave conditions at the main study sites. *A,* Close to the surface. *B,* Close to the seabed. The principal axes were oriented more sub-parallel to the isobaths. The mean current direction during large wave events was offshore at most of the instrument sites.

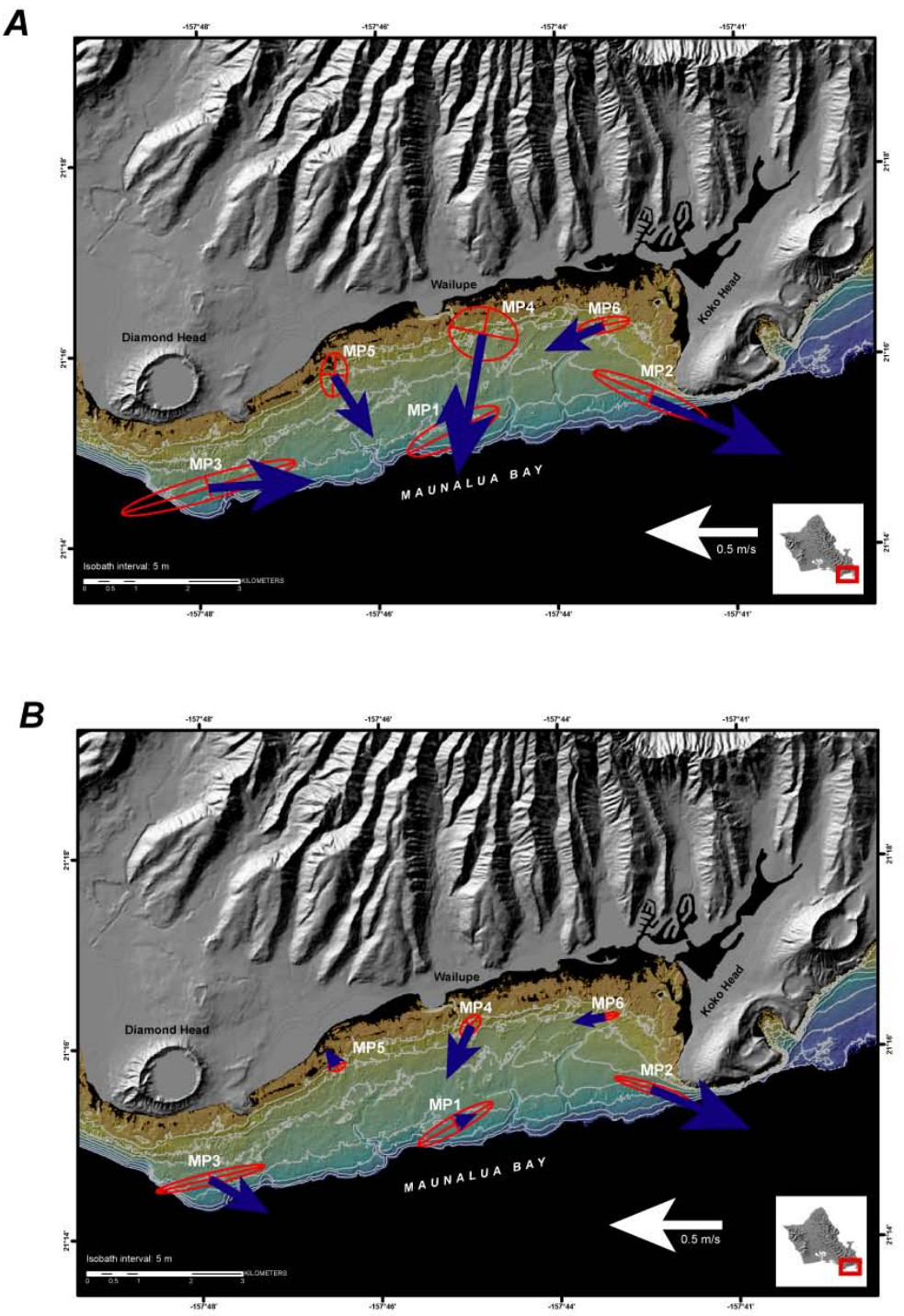

FIGURE 20. Principal axis ellipses and mean current speeds and directions, in meters per second from degrees true north, during the Decemeber 11, 2008 (2008 Year Day 346), Kona storm at the main study sites. *A,* Close to the surface. *B,* Close to the seabed. The principal axes were oriented alongshore to the east off Koko Head and Diamond Head, onshore in the deep middle portion of the bay, and primarily offshore from the shallow northern portion of the bay. Together, this suggests that flow primarily was offshore to the west along the fringing reef's fore reef and then to the east over the outer, deeper portion of the bay.

FIGURE 21. Photographs, looking south, of the eastern portion of Maunalua Bay taken by the Terrestial Imaging System (TIS) during the December 10-12, 2008 Kona storm (2008 Year Day 345-347). *A,* Image taken on the evening of December 10, 2008 (2008 Year Day 345), showing strong onshore southerly winds. *B,* Image taken on the morning of December 11, 2008 (2008 Year Day 346), showing heavy precipitation and large waves breaking along and offshore of the reef crest. *C,* Image taken midday on December 11, 2008 (2008 Year Day 346), showing large waves breaking along and offshore of the reef crest, apparently resuspendeding large quantities of carbonate sediment as infered by the light color of the water; also visible is a plume of terrestrial sediment stretching along the coast from Paiko Lagoon east around to the western flank of Koko Head, and extending from there along the reef crest west past Paiko Lagoon. *D,* Image taken late in the day on December 11, 2008 (2008 Year Day 346), showing decreasing wave heights and less carbonate sediment resuspension but with the plume of terrestrial sediment extending much further offshore on the fore reef to the west past Paiko Lagoon.

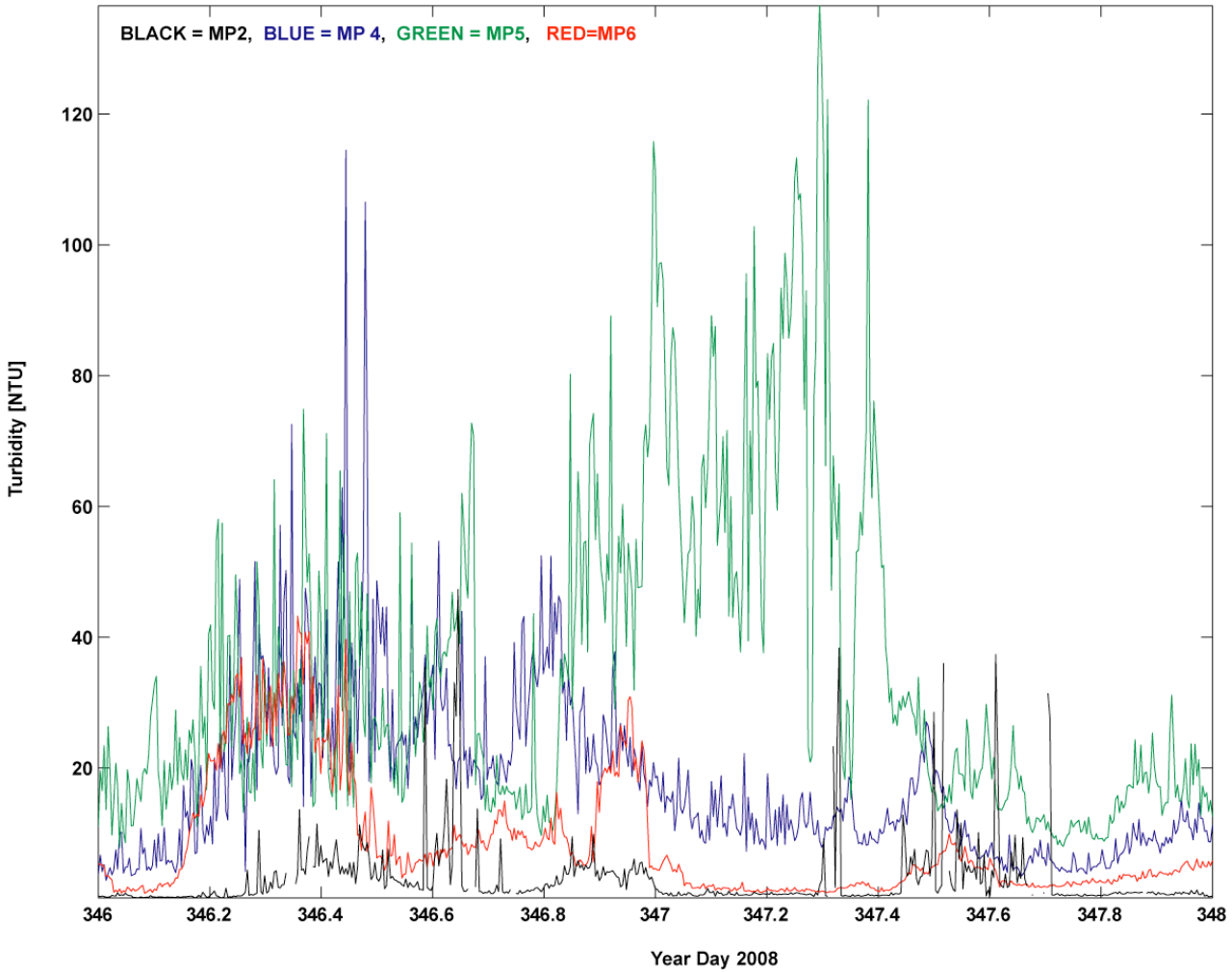

FIGURE 22. Turbidity, in Nephelometric Turbidity Units, during the December 10-12, 2008 (2008 Year Day 346-348), Kona storm. The largest increase and duration in turbidity was observed at site MP5, with maximum values exceeding 120 NTU and turbidity values greater than 35 NTU for more than 1065 min; the turbidity values exceeded 35 NTU for 50 min at site MP6 and 310 min at site MP4.

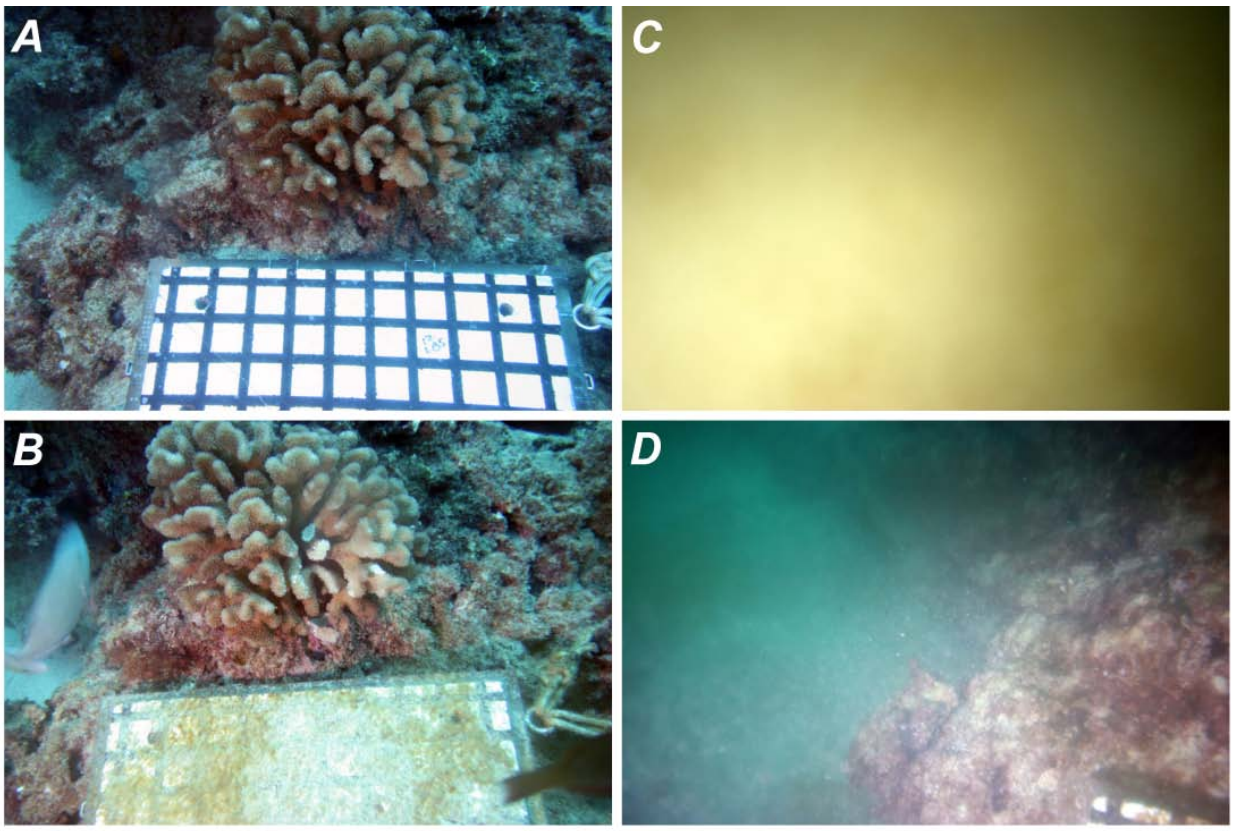

FIGURE 23. Photographs of a coral head and calibration block at site MP6 in northeastern Maunalua Bay taken by the Coral Imaging System (CIS). *A,* Image taken just after deployment in November 2008 showing the position of the camera's field of view relative to the coral head, reef structure, calibration block, and sand-covered sea floor. *B,* Image taken just before the Kona storm on December 9, 2008 (2008 Year Day 344), showing algae that has grown on the calibration block and a small change in perspective due to settling of one of the CIS tripod's legs. *C,* Image taken at midday on December 11, 2008 (2008 Year Day 346) during the Kona storm, showing the extremely high turbidity (as shown by the almost complete blackness in the right side of the image away from the strobe's illumination on the left) that is reddish-brown in color, suggesting a terrestrial source. *D,* Image taken on December 13, 2008 (2008 Year Day 348) after the Kona storm, showing the CIS tripod had been rotated so much by wave forces that the coral head is no longer in the field of view. Note the much lighter (whiter) color of the material in suspension, suggesting the sediment was carbonate material resuspended from the seabed by waves and thus the terrestrial sediment imaged during the storm was no longer prevelant in the water column.

present at that part of the bay. The inshore sites also showed little change in temperature during this time period (fig. 24*C*). Conversely the salinity signal at sites MP4, MP5, and MP6 showed large decreases in salinity during this period. The salinity values were lower than 25 PSU (as discussed above, mean for bay ~35 PSU) for 70 min at site MP4 and 85 min at site MP6, indicating the presence of freshwater either from surface runoff in the form of a freshwater plume being mixed down close to the seabed by the large waves or submarine groundwater discharge (SGD).

Spatial Variability in Turbidity and Salinity

The spatial variability for salinity shows the mean and the standard deviation at each site (fig. 25a). The highest salinity values were measured in the eastern portion of the bay and the lowest values in the west, loosely mirroring the terrestrial east-west gradient in rainfall and groundwater recharge, with the Ko'olau Range bordering the northwestern part of the bay receiving more than twice the

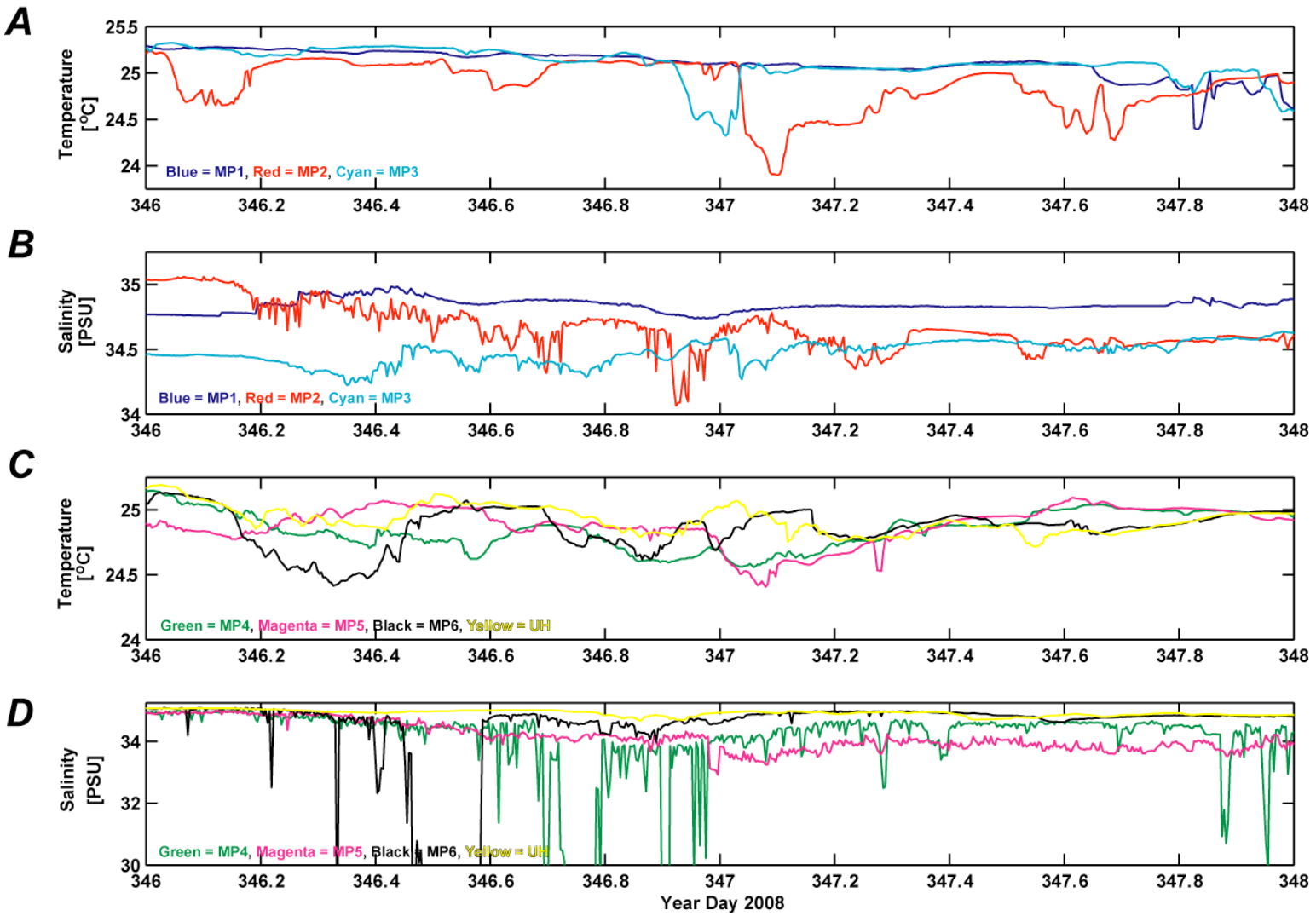

FIGURE 24. Temperature and salinity data during the December 10-12, 2008 (2008 Year Day 346-348), Kona storm. *A,* Temperature at the deep and shallow sites, in degrees Celcius. *B,* Salinity at the deep and shallow sites, in Practical Salinity Units. A large decrease in salinity was observed at the Wailupe (MP4) and Paiko (MP6) sites, indicative of a large input of fresh water.

precipitation than at Koko Head in the east. The areas of lower salinity values and higher variability were in the western part of the bay near sites MP4 and MP5. These locations may have a greater influence of freshwater surface flow and SGD. Site MP2 near Koko Head on the eastern edge of the bay also had lower salinity values that suggest the possible influence of SGD.

The spatial variability for turbidity shows the mean and the standard deviation at each site (fig. 25b). The highest mean and standard deviation of turbidity values were measured at sites MP4 and MP5; the eastern portion of the bay showed low mean turbidity values with very little variation. The highest turbidity values were measured closer to shore and were greater in the western portion of the bay, either indicating a westward transport of sediment along the bay's fringing reef and/or greater inputs of sediment to the bay by the streams in the Kahala region due to higher rainfall upslope in the Ko'olau Range.

Overall, the data from the time-series measurements at the instrument sites and the water-column surveys suggest that the Hawaii Kai Harbor channel and northeastern portion of the bay is much different in nature compared to the rest of Maunalua Bay. This is likely due to three reasons. First, the Hawaii Kai Harbor channel is relatively confined, being incised 3-5 m deep in the 0.5-1.5 m deep reef flat that dominates the northeastern portion of the bay between Paiko Lagoon and Koko Head. Second, the northeastern portion of the bay is in the lee of Koko Crater and Koko Head, and thus is subjected to relatively lower trade-wind speeds as compared to the western portion of the bay. Lastly, the channel drains the marina, which has different water properties than the bay. As a result of the confined nature of the channel and relatively limited trade-wind forcing in the area (wind-driven currents and trade-wind waves), it appears that the Hawaii Kai Harbor channel incised into the reef-flat and the northeastern portion of the bay is mixed relatively poorly and therefore characterized by water-column properties unlike those that dominate the majority of the fore reef and deeper waters through the rest of the bay.

Sediment Dynamics

By comparing the critical shear stress (amount of stress, or force applied per unit area) for the sediment on the seabed and the sediment collected in the sediment traps at each site to the shear stress applied to the seabed by waves and currents at each site, an understanding of the frequency that the material at a given site is mobilized and resuspended can be determined. When the critical shear stress for sediment is less than wave- and current-induced shear stresses, the sediment is in motion; conversely, when the critical shear stress is greater than the applied wave and current shear stresses, the sediment either falls out of suspension and settles (sedimentation) or is not mobilized from the seabed. During this study, the finer material collected in the sediment traps at all of the main study sites (fig. 26) was more frequently (51.8%) in motion than the coarser material on the seabed (36.4%). The high current speeds at the deeper (~20 m depth) sites off Koko Head and Diamond Head result in greater percentages of time the seabed (72.4±5.9%) and sediment trap (87.2±12.0%) material was in motion compared to the percentages determined for sediment at the shallower (<10 m depth) sites (12.5±11.8% and 28.2±7.9%, respectively). The lower frequency of motion at the shallower sites in the bay suggest a greater probability of greater temporary sedimentation of similar-sized material at these sites compared to those further offshore along the 20 m isobath.

Cumulative sediment flux is the mass of sediment moving through an area during a particular time period, and it shows in which locations the most (or least) sediment is transported through the area due to the mean current velocities and suspended-sediment concentrations (SSC). Instantaneous sediment fluxes were calculated using the SSCs calculated from the SLOBS turbidity data (appendix 7) and the near-bed velocity data collected from the ADCP's lowest bin; these instantaneous fluxes were

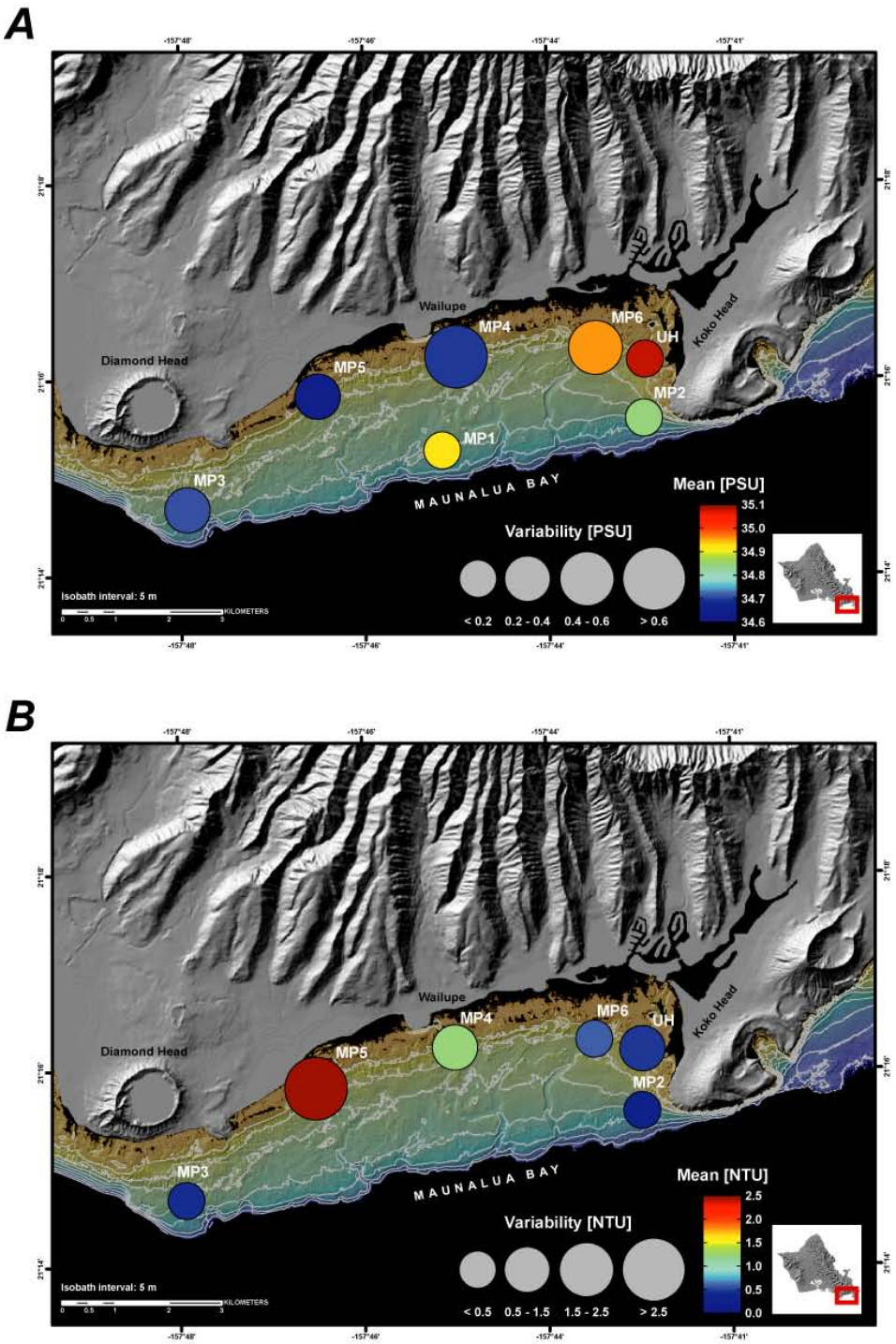

FIGURE 25. Mean and variability in salinity and turbidity at the main study sites. Variability in temperature and salinity variability at the instrument sites. *A,* Salinity, in Practical Salinity Units. *B,* Turbidity, in Nephelometric Turbidity Units. The shallow, north-central (Wailupe, site MP4) and northwestern (Kahala, site MP5) portions of the bay generally are lower in salinity and more turbid than elsewhere in the bay and appear to be areas where fresher, sediment-laden water enters the bay. The shallow, northeastern (Hawaii Kai sites MP6 and MP8) portion of the bay generally has lower turbidities and higher salinities than observed to the west.

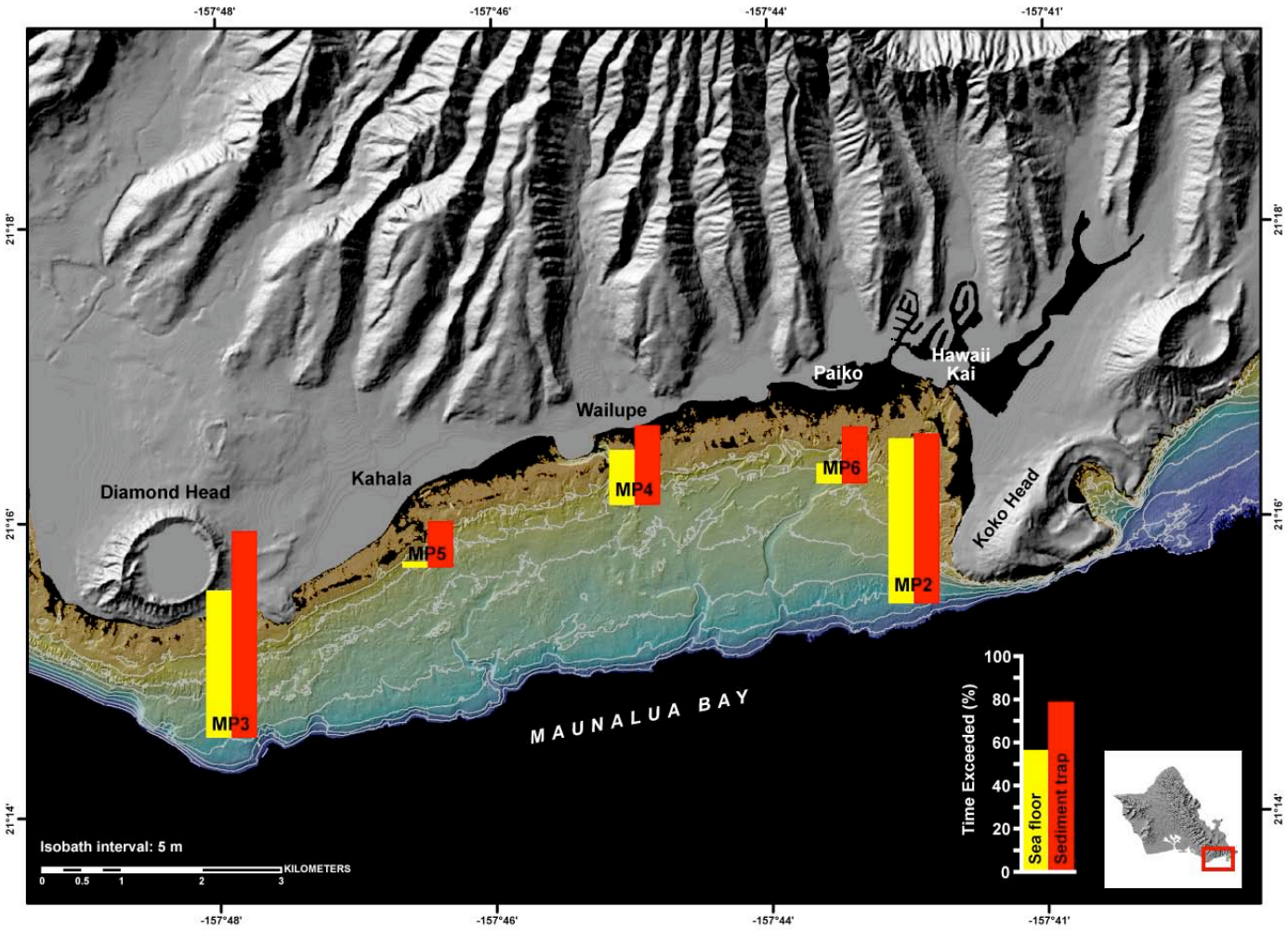

FIGURE 26. Frequency of sediment mobility, in percentage of time during the experiment, at the main study sites. The plot shows the percentage of time that the critical shear stress for the sediment on the sea floor (yellow) and collected in the sediment traps (red) at the site was exceeded by the wave- and current-induced shear stresses at the site, and thus the sediment was in motion. In all cases, the finer material collected in the sediment traps was more frequently in motion than the coarser material on the sea floor. The strong current speeds at the deeper (~20 m depth) sites off Koko Head and Diamond Head result in greater percentages of time the sea floor and sediment trap material was in motion compared to the shallower (<10 m) sites. The lower frequency of motion at the shallower sites in the bay suggests a greater probability of longer temporary sedimentation of similar-sized material at these sites compared to those further offshore.

then summed for the period of calculation. Due to instrument problems, SSC data were collected only for 2008 Year Days 315-325 (November 10-20, 2008) at all of the instrument sites (table 14). For this time period, the largest mass of sediment (52.48 kg/cm^2) in the bay was transported offshore to the southeast at site MP5 off Kahala (fig. 27a) due to a combination of moderate near-bed current velocities and relatively high SSCs. The orientation to the southeast is in contrast to the dominant westward flow pattern under trade-wind forcing (fig. 18) and suggests that there is strong coupling between tides and SSCs, with higher SSCs occuring during falling tides when flow is predominantly to the southeast (fig. 17). Similar patterns of higher SSCs during falling tides have been observed along fringing reefs off south Molokai (Storlazzi et al., 2004) and west Maui (Storlazzi and Jaffe, 2008), where terrestrial sediment deposited on the reef flat was resuspended by larger waves and stronger currents at high tide and advected off the reef flat and over the fore reef as the falling tides drained the sediment-laden water off the reef flats. While characterized by vigorous near-bed current velocities, relatively little sediment was transported offshore at the deeper (~20 m depth) sites in the bay due to the very low SSCs. Overall, the predominant direction of near-bed sediment flux through the bay was offshore toward the southeast and the sites closer to shore (MP4, MP5, and MP6) exhibited the greatest near-bed sediment fluxes in the bay, with decreasing quantities from west to east.

Although not all of the SLOBS were operational for the entire study period, the inshore instruments collected data during 2008 Year Days 315-396 (November 10, 2008 – January 30, 2009) and provide a picture of the amount of sediment moving through the bay during the experiment. As during the period when all the instruments were functioning properly (2008 Year Days 315-325), the greatest near-bed sediment flux (2680.05 kg/cm^2) occurred at site MP5 off Kahala; the sediment flux decreased toward the east, with 519.03 kg/cm^2 of sediment flux at site MP6 off Paiko Lagoon (fig 27b). Similar to the predominant direction of near-bed sediment flux during the limited time when all of the instruments were working, the sediment flux at all of the shallow (<10 m depth) sites for the entire experiment was offshore toward the southeast, and the coupling between high SSCs and falling tides is apparent. These values were two orders of magnitude greater than the fluxes measured during the first 10 days of the experiment. This can be attributed partially to the large storm waves, precipitation, and fluvial discharge during the December 10-12, 2008 (2008 Year Day 345-347), Kona storm that delivered large quanties of sediment to the bay.

These calculations, together with the large quanity of in place and remotely-sensed data from this experiment, suggest that most of the terrestrial sediment that enters the bay from the northern shoreline is driven westward on the reef flats along the northern part of the bay. Any sediment that is carried offshore of the reef flats by larger plumes likely is advected rapidly offshore to the southeast due to the high current velocities in the deeper portions of the bay. As the sediment-laden water on the reef flat is advected off the reef flat due to combinations of winds, waves, and falling tides, temporary depostion on the shallow fore reef in the northern portion of the bay likely occurs due to the low shear stresses. There is little to no long-term accumulation of this terrestrial sediment, and it is advected quickly offshore and dispersed. Thus, the inner bay's reef flats and shallow fore reefs likely are subjected to high turbidity values following input events and possibly temporary, short-duration sediment deposition but not long-term accumulation of sediment. Due to their more energetic nature, the outer portions of the bay are subjected to neither these high turbidity nor temporary depostion events. Overall, although significant volumes of terrigenous sediment may be delivered to Maunalua Bay, these particles likely are advected through the bay's waters relatively quickly and do not reside on the seabed for long durations. Although this fine-grained terrestrial sediment was not observed on the seabed during this study or incorporated in large amounts into the geologic record, it was advected over the

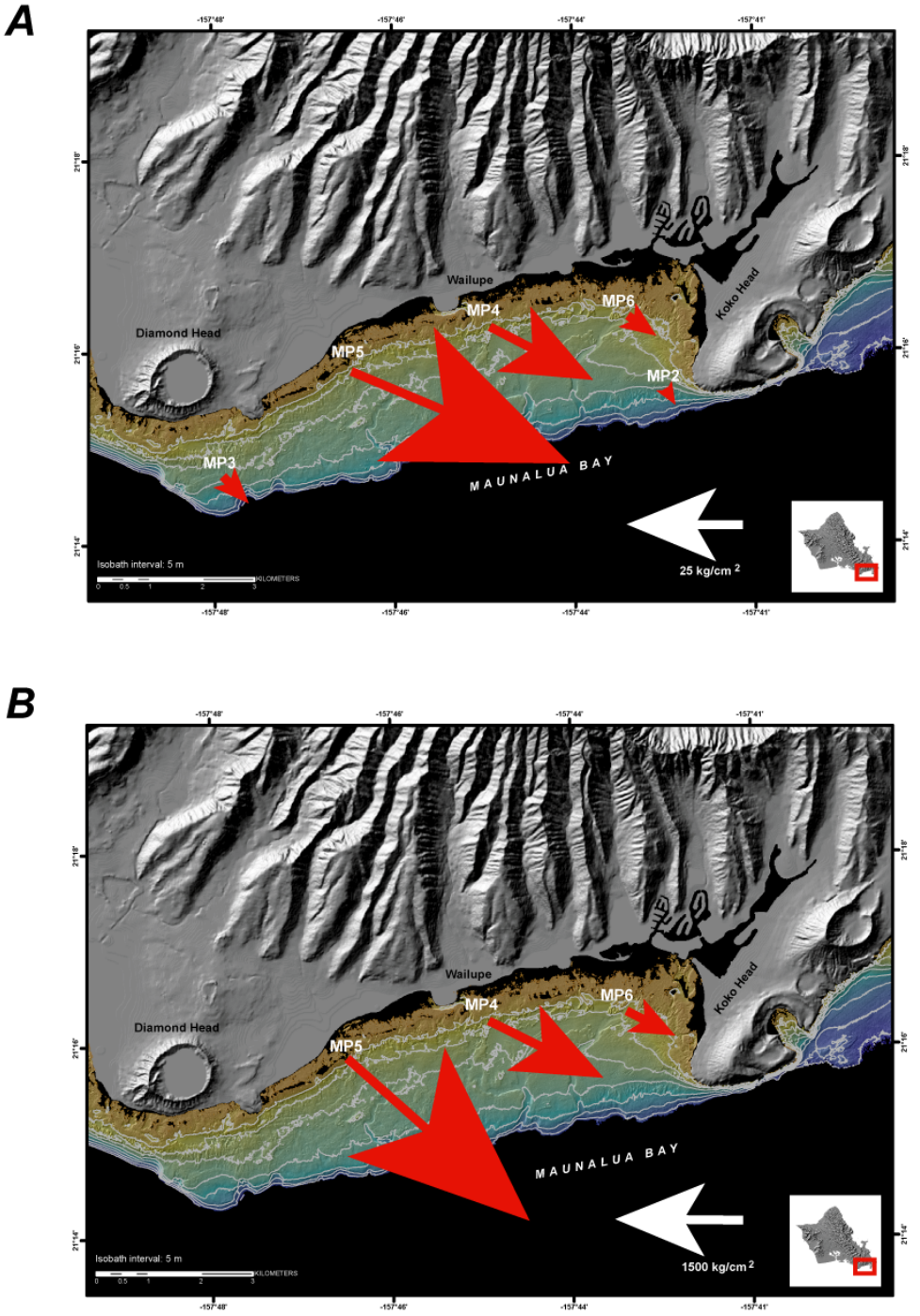

FIGURE 27. Cumulative near-bed sediment fluxes at the main study sites. *A*, 2008 Year Days 315-325 when all of the instruments were functioning properly. *B*, 2008 Year Days 315-396 that encompassed the entire study period. Note the change in scale between *A* and *B*.Overall, the predominant direction of near-bed sediment flux through the bay was offshore towards the southeast. The sites closer to shore (MP4, MP5, and MP6) exhibited the greatest near-bed sediment fluxes in the bay, with decreasing quantities from west to east, similar to the gradient in turbidity values as shown in figure 26. The values shown for the entire study period were two orders of magnitude greater than the fluxes measured during the first 10 days of the experiment; this can partially be attributed to the large storm waves, precipitation, and fluvial discharge during the December 10-12, 2008 (2008 Year Day 345-347), Kona storm that delivered large quanties of sediment to the bay.

bay's fringing reefs, and has the potential consequence of decreasing photosynthetically available radiation (PAR) and desorbing nutrients and/or contributing toxicants. Some researchers (e.g., Marszalek, 1981) suggest that prolonged turbidity and the resulting decreased photosynthetically available radiation (PAR) are more detrimental to corals than short-term accumulation of sediment.

Conclusions

More than 2.6 million measurements of meteorologic and oceanographic forcing and the resulting water-column properties were made. Key findings from these measurements and analyses include the following.

1. Due to the wide range of conditions observed during this experiment, we were able to sufficiently characterize the different combination of atmospheric and oceanographic forcing conditions typically observed in the Hawaiian Islands. Circulation in the bay was primarily to the west due to the prevalent trade-wind forcing. Tidal circulation was to the west (counter-clockwise) during flood tide and to east (clockwise) during ebb tide. Large south swell events that impacted the bay appear to flush the bay by driving flow primarily offshore.
2. Overall, turbidity was relatively low in the bay during the entire study. The most turbid periods occurred after heavy precipitation and run-off and/or resuspension from large waves. The turbidity decreased quickly to pre-event levels upon the cessation of forcing (fluvial discharge or large waves), likely due either to the fast current speeds that advected finer material out of the bay or the rapid settling of the sand-sized particles (carbonate material that dominates the seabed in the bay).
3. In comparison with areas elsewhere in the bay, the shallow, north-central (off Wailupe) and northwestern (off Kahala) portions of the bay generally are lower in salinity and more turbid and appear to be areas where fresher, sediment-laden water enters the bay. The shallow, northeastern (off Hawaii Kai) portion of the bay generally has lower turbidity values and higher salinity values than are observed in areas to the west. The salinity and turbidity data suggest one of the following: (1) sediment and freshwater inputs are greatest in the central and western portions of the bay, causing the fore reef in these regions to be most directly impacted by depressed salinity values and elevated turbidity values; or (2) while sediment may be introduced at many points along the bay's northern shoreline, including the Hawaii Kai region, westward transport along the northern bay's reef flat by the northeast trade winds results in depressed salinity values and elevated turbidity values along the fore reef coral habitats along the central and western portions of the bay. Furthermore, the data from the in place time-series measurements at the instrument sites and the water-column surveys suggest that the Hawaii Kai region and northeastern portion of the Maunalua Bay is characterized by water-column properties unlike those that dominate the majority of the fore reef and deeper waters through the rest of the bay.
4. The December 10-12, 2008, Kona storm introduced large quantities of freshwater and terrigenous sediment into Maunalua Bay that resulted in high (>35 NTU) turbidity values and significantly depressed (<25 PSU) salinity values for hours at the inner bay sites. Although turbidity levels were elevated, it is evident from the sediment traps and seabed samples that this terrigenous sediment did not reside in the bay and apparently was advected away from the sites where measurements were made.

5. The lower frequency of sediment motion at the shallower (<10 m depth) sites in the bay suggests a greater probability of temporary deposition compared to deeper areas (20 m). Overall, the dominant direction of near-bed sediment flux through the bay was offshore toward the southeast. The shallower sites (<10 m) exhibited the greatest near-bed sediment fluxes in the bay, with decreasing quantities from west to east. Although significant volumes of terrigenous sediment may be delivered to Maunalua Bay, these particles likely are advected through the bay's waters relatively quickly and probably do not reside on the seabed for long durations. Although fine-grained terrestrial sediment was not observed on the seabed during this study, it was advected over the bay's fringing coral reefs where it had the potential for decreasing photosynthetically-available radiation (PAR) and for desorbing nutrients and/or contributing toxicants.

These data provide information on the nature and controls on flow and water-column properties in Maunalua Bay, Oahu, during winter conditions. A number of interesting phenomena were observed that indicate the complexity of coastal circulation and sediment dynamics in the bay and may help to better understand the implications of the processes on coral reef health.

Acknowledgments

This work was carried out as part of the USGS's Coral Reef Project as part of an effort in the United States and its trust territories to better understand the affect of geologic processes on coral reef systems. Robert Richmond (UH), Jonathan Martinez (UH), and the staff at the University of Hawaii's Kewalo Marine Laboratory helped with project planning and provided significant logistical help and facilities to support our field operations. Alyssa Miller (Malama Maunalua) and others at Malama Maunalua helped with local project coordination and outreach. Gordon Tribble and Ron Rickman (USGS-WRD) provided field support and scientific insight while also helping with project coordination. Richard Boyd, the manager at Mt. Terrace Condominiums, provided us with access and security that made it possible to deploy our Terrestrial Imaging System and weather station atop his facility. Mike Torresan (USGS) and Angela Lam (USGS) processed the sediment samples described in this report. We would also like to thank Bruce Richmond (USGS) and Jeff Hansen (USGS) who contributed numerous excellent suggestions and a timely review of our work.

References Cited

Baker, E.T., Milburn, H.B., and Tennant D.A., 1988, Field assessment of sediment trap efficiency under varying flow conditions: Journal of Marine Research, v. 46, p. 573-592.

Barber, S.G., 2002, Laboratory procedures and grain size analysis of terrigenous and carbonaceous sediment of the fringing reef of Molokai, Hawaii: California, San Francisco State University, thesis, p. 4-13, appendix A.

Bothner, M.H., Reynolds, R.L., Casso, M.A., Storlazzi, C.D., and Field, M.E., 2006, Quantity, composition, and source of sediment collected in sediment traps along the fringing coral reef off Molokai, Hawaii: Marine Pollution Bulletin, v. 52, p. 1034–1047.

Department of Health, Office of Environmental Quality Control, State of Hawaii, 2004, Hawaii Administrative Rules: Amendment and Compilation of Chapter 11-54, 64 p. [*http://oeqc.doh.hawaii.gov/sites/har/AdmRules1/11-54.pdf*] *(last accessed February, 15, 2010).*

Gardner, W.D., Richardson, M.J., Hinga, K.R. and Biscaye, P.E., 1983, Resuspension measured with sediment traps in a high-energy environment: Earth and Planetary Science Letters, v. 66, p. 262-278.

Marszalek, D.S., 1981, Impact of dredging on a subtropical reef community--Southeastern Florida, U.S.A: Proceedings of the 4th International Coral Reef Congress, p. 147-153.

National Water Information System (NWIS), 2010. Station 211722157485601 H-1 storm drain at Kapiolani Ave, Oahu, HI, data: U.S. Geological Survey [*http://waterdata.usgs.gov/usa/nwis/uv?211722157485601*] *(last accessed February, 15, 2010).*

Phillip, E., and Fabricius, K.E., 2003, Photophysiological stress in scleractinian corals in response to short-term sedimentation: Journal of Experimental Marine Biology and Ecology, v. 287, p. 57-78.

Presto, M.K., Ogston, A.O., Storlazzi, C.D., and Field, M.E., 2006, Temporal and spatial variability in the flow and dispersal of suspended-sediment on a fringing reef flat, Molokaʻi, Hawaiʻi: Estuarine Coastal and Shelf Science, v. 67, p. 67-81.

Storlazzi, C.D. and Jaffe, B.E., 2008, The relative contribution of processes driving variability in flow, shear, and turbidity over a fringing coral reef--West Maui, Hawaii: Estuarine Coastal and Shelf Science, v. 77, no. 4, p. 549-564.

Storlazzi, C.D., Ogston, A.S., Bothner, M.H., Field, M.E., and Presto M.K., 2004, Wave- and tidally-driven flow and sediment flux across a fringing coral reef--South-central Molokai, Hawaii: Continental Shelf Research, v. 24, no. 12, p. 1397-1419.

Additional Digital Information

For additional information on the instrument deployments, please see:
http://walrus.wr.usgs.gov/infobank/a/a1108oa/html/a-11-08-oa.meta.html
http://walrus.wr.usgs.gov/infobank/a/a209oa/html/a-2-09-oa.meta.html

For an online PDF version of this report, please see:
http://pubs.usgs.gov/of/2010/1217/

For more information on the U.S. Geological Survey Western Region's Coastal and Marine Geology Team, please see:
http://walrus.wr.usgs.gov/

For more information on the U.S. Geological Survey's Coral Reef Project, please see:
http://coralreefs.wr.usgs.gov/

Direct Contact Information

General Project Information
Michael E. Field (USGS Coral Reef Project chief): *mfield@usgs.gov*

Regarding this Report:
Curt D. Storlazzi (Lead oceanographer): *cstorlazzi@usgs.gov*

Table 1. Experiment Personnel.

Person	Affiliation	Responsibilities
Mike Field	USGS	Chief Scientist, diver
Curt Storlazzi	USGS	Co-chief scientist, diver
Kathy Presto	USGS	Oceanographer, Instrument specialist
Joshua Logan	USGS	Information specialist, diver
Tom Reiss	USGS	Dive safety officer
Henry Chezar	USGS	Imaging technician
Randy Russell	USGS	Field and IT support technician
Joe Reich	*F/V Alyce C*	Vessel captain

Table 2. Instrument Package Sensors.

Site Name	Depth [m]	Sensors
MP1	22	Nortek 600 kHz AWAC acoustic Doppler current profiler
	22	Seabird SBE-37SI Microcat conductivity-temperature sensor
MP2	20	RD Instruments 600 kHz Workhorse Monitor acoustic Doppler current profiler
	20	Aquatec/Seapoint 200-TY optical backscatter sensor
	20	Seabird SBE-37SI Microcat conductivity-temperature sensor
	20	Sediment tube trap
MP3	20	RD Instruments 600 kHz Workhorse Monitor acoustic Doppler current profiler
	20	Aquatec/Seapoint 200-TY optical backscatter sensor
	20	Seabird SBE-37SI Microcat conductivity-temperature sensor
	20	Sediment tube trap
MP4	9	Nortek 2000 kHz Aquadopp acoustic Doppler current profiler
	9	Aquatec/Seapoint 210-TYT optical backscatter sensor
	9	Seabird SBE-37SI Microcat conductivity-temperature sensor
	9	Sediment tube trap
MP5	9	Nortek 2000 kHz Aquadopp acoustic Doppler current profiler
	9	Aquatec/Seapoint 210-TYT optical backscatter sensor
	9	Seabird SBE-37SI Microcat conductivity-temperature sensor
	9	Sediment tube trap
MP6	8	RD Instruments 600 kHz Workhorse Monitor acoustic Doppler current profiler
	8	Aquatec/Seapoint 210-TYT optical backscatter sensor
	8	Seabird SBE-37SI Microcat conductivity-temperature sensor
	8	Sediment tube trap
	8	USGS Coral Imaging System (CIS)
UH	5	Aquatec/Seapoint 210-TYT optical backscatter sensor
	5	Seabird SBE-37SI Microcat conductivity-temperature sensor
Weather Station (WS) [10]	[71]*	NovaLynx WS-16N-A weather station
Terrestial Imaging System (TIS) [12]	[71]*	USGS Terrestrial Imaging System

*Height, in meters

Table 3. Instrument Package Location Information.

Site Name	Latitude [decimal degrees]	Longitude [decimal degrees]
MP1	21.25416	-157.72467
MP2	21.25989	-157.71616
MP3	21.24471	-157.79857
MP4	21.27082	-157.74967
MP5	21.26383	-157.77490
MP6	21.27194	-157.72472
UH	21.26658	-157.71772
Weather Station (WS)	21.28777	-157.71938
Terrestial Imaging System (TIS)	21.28758	-157.71944
USGS stream gauge	21.28944	-157.81555

Table 4. Water-Column Profiler Cast Location and Depth Information.

Cast Number/Site	Latitude [decimal degrees]	Longitude [decimal degrees]	Depth [m]
1	-157.79820	21.24400	19.9
2	-157.80016	21.24809	12.2
3	-157.79985	21.25112	9.5
4	-157.77017	21.25021	21.3
5	-157.74876	21.25558	19.5
6	-157.73181	21.25807	18.6
7	-157.71502	21.25971	19.8
8	-157.71805	21.26598	7.9
9	-157.71607	21.27085	4.9
10	-157.71440	21.27455	0.9
11	-157.71360	21.27632	4.6
12	-157.71305	21.27774	4.3
13	-157.71338	21.27884	3.7
14	-157.71180	21.28114	1.7
15	-157.72521	21.27286	5.5
16	-157.73001	21.26533	14.0
17	-157.73428	21.27334	7.3
18	-157.74930	21.27100	6.1
19	-157.75042	21.26298	14.9
20	-157.76071	21.26722	8.2
21	-157.77315	21.25671	14.3
22	-157.77450	21.26349	9.5
23	-157.78641	21.25703	8.2

Table 5. Meteorological Statistics.

[All statistics were calculated for 2008 Year Days 315-413; wind direction is "Going to"]

Site Name	Mean ± 1 Std Deviation	Minimum	Maximum
Sea level barometric pressure [mb]	1008.40±2.60	998.31	1020.38
Air temperature [°C]	22.97±1.55	17.75	29.31
Precipitation [mm]	0.05±0.40	0	10.25
Wind speed [m/s]	4.77±2.83	0	15.75
Wind direction [°]	105.2±84.7	0.2	359.6

Table 6. Wave Statistics.

[All statistics were calculated for 2008 Year Days 315-413; wave direction is "From"]

Site Name	Parameter	Mean ± 1 Std Deviation	Minimum	Maximum
MP1	Height [m]	1.06 ±0.34	0.48	4.07
	Period [s]	4.35±0.63	2.24	6.68
	Direction [°]	146.1±17.2	109.4	216.1
MP2	Height [m]	0.96±0.37	0.40	7.01
	Period [s]	6.04±0.68	2.6	9.7
	Direction [°]	157.0±23.1	107.0	249.0
MP3	Height [m]	0.94±0.31	0.41	3.41
	Period [s]	6.31±0.75	4.3	9.0
	Direction [°]	161.1±35.8	79.0	269.0
MP4	Height [m]	1.01±0.33	0.43	3.31
	Period [s]	4.42±0.63	2.93	8.06
	Direction [°]	162.4±22.6	96.9	268.5
MP5	Height [m]	1.05±0.36	0.41	3.09
	Period [s]	4.08±0.51	3.09	7.02
	Direction [°]	132.0±17.8	38.3	313.3
MP6*	Height [m]	0.72±0.27	0.35	2.64
	Period [s]	5.71±0.78	3.9	9.3
	Direction [°]	179.1±14.3	139.0	239.0

*Statistics were calculated only for 2008 Year Days 315-388.

Table 7. Current Statistics.

[All statistics were calculated for 2008 Year Days 315-413; current direction is "Going to"]

Site Name	Parameter	Depth [m]	Mean ± 1 Std Deviation	Minimum	Maximum
MP1	Speed [m/s]	2	0.24±0.14	0.00	0.94
	Direction [°]	2	159.9±100.2	0.0	359.9
	Speed [m/s]	21	0.18±0.10	0.00	0.74
	Direction [°]	21	155.8±93.7	0.0	359.9
MP2	Speed [m/s]	2	0.30±0.16	0.00	1.01
	Direction [°]	2	184.9±81.4	14.2	358.7
	Speed [m/s]	19	0.20±0.11	0.00	0.65
	Direction [°]	19	187.9±84.1	14.3	359.5
MP3	Speed [m/s]	2	0.44±0.23	0.01	1.07
	Direction [°]	2	165.5±83.8	6.1	359.7
	Speed [m/s]	19	0.26±0.14	0.01	0.71
	Direction [°]	19	164.6±80.6	0.8	358.6
MP4	Speed [m/s]	2	0.34±0.19	0.01	2.18
	Direction [°]	2	193.2±64.7	0.0	359.9
	Speed [m/s]	8	0.06±0.04	0.00	0.27
	Direction [°]	8	162.1±81.5	0.0	359.5
MP5	Speed [m/s]	2	0.19±0.12	0.00	1.99
	Direction [°]	2	178.5±70.4	0.0	359.9
	Speed [m/s]	8	0.04±0.03	0.00	0.24
	Direction [°]	8	191.7±83.9	0.0	359.9
MP6*	Speed [m/s]	2	0.10±0.06	0.00	0.42
	Direction [°]	2	156.0±92.5	0.0	359.7
	Speed [m/s]	7	0.06±0.03	0.00	0.27
	Direction [°]	7	143.6±86.7	0.5	359.7

*Statistics were calculated only for 2008 Year Days 315-388.

Table 8. Temperature Statistics.

[All statistics were calculated for 2008 Year Days 315-356]

Site Name	Depth [m]	Mean ± 1 Std Deviation [°C]	Minimum [°C]	Maximum [°C]
MP1	22	24.32±0.39	23.71	26.19
MP2	20	25.25±0.38	23.73	26.08
MP3	20	25.34±0.40	23.89	26.24
MP4	9	25.19±0.40	23.94	26.28
MP5	9	25.11±0.48	23.65	26.36
MP6	8	25.20±0.41	23.87	26.18
UH	5	25.30±0.37	24.49	26.17

Table 9. Salinity Statistics.

[All statistics were calculated for 2008 Year Days 315-356]

Site Name	Depth [m]	Mean ± 1 Std Deviation [PSU]	Minimum [PSU]	Maximum [PSU]
MP1	22	34.92±0.11	34.35	35.16
MP2	20	34.83±0.17	34.07	35.13
MP3	20	34.71±0.19	34.22	35.13
MP4	9	34.69±0.73	19.64	35.09
MP5	9	34.63±0.38	32.92	35.07
MP6	8	34.94±0.55	22.99	35.18
UH	5	35.07±0.08	34.62	35.21

Table 10. Turbidity Statistics.

[All statistics were calculated for 2008 Year Days 315-325]

Site Name	Depth [m]	Mean ± 1 Std Deviation [NTU]	Minimum [NTU]	Maximum [NTU]
MP2	20	0.21±0.20	0.09	5.96
MP3	20	0.39±0.27	0.15	2.28
MP4	9	1.19±1.20 [1.72±3.64]*	0.34 [0.21]*	11.36 [114.47]*
MP5	9	2.43±3.60 [5.54±7.44]*	0.41 [0.41]*	31.94 [136.57]*
MP6	8	0.54±0.46 [0.80±1.98]*	0.21 [0.16]*	5.38 [43.24]*
UH	5	0.46±0.85	0	10.03

*Additional statistics were calculated for 2008 Year Days 315-396.

Table 11. Sediment Sample Location and Depth Information.

USGS Sample Identifier	Site Name	Sample Type	Average Trap Collection Rate [mg/cm^2/day]	Latitude [decimal degrees]	Longitude [decimal degrees]	Depth [m]
OA-0209-SF2	MP-2	Sea floor	-	21.25989	-157.71616	20
OA-0209-SF3	MP-3	Sea floor	-	21.24471	-157.79857	20
OA-0209-SF4	MP-4	Sea floor	-	21.27082	-157.74967	9
OA-0209-SF5	MP-5	Sea floor	-	21.26383	-157.77490	9
OA-0209-SF6	MP-6	Sea floor	-	21.27194	-157.72472	8
OA-0209-TP2	MP-2	Sediment trap	63.49	21.25989	-157.71616	20
OA-0209-TP3	MP-3	Sediment trap	10.22	21.24471	-157.79857	20
OA-0209-TP4	MP-4	Sediment trap	126.35	21.27082	-157.74967	9
OA-0209-TP5	MP-5	Sediment trap	206.49	21.26383	-157.77490	9
OA-0209-TP6	MP-6	Sediment trap	80.40	21.27194	-157.72472	8

Table 12. Sediment sample grain size Information.

USGS Sample Identifier	Gravel [percent]	Sand [percent]	Silt [percent]	Clay [percent]	Mud [percent]	Mean Size [mm]
OA-0209-SF2	0.47	98.93	0.33	0.28	0.60	0.205
OA-0209-SF3	19.58	79.81	0.34	0.26	0.60	0.744
OA-0209-SF4	0.00	99.67	0.18	0.15	0.33	0.341
OA-0209-SF5	2.56	97.12	0.14	0.17	0.31	0.479
OA-0209-SF6	0.64	99.36	0.00	0.00	0.01	0.792
OA-0209-TP2	0.05	96.36	2.45	1.14	3.59	0.176
OA-0209-TP3	0.25	73.59	19.19	6.97	26.16	0.069
OA-0209-TP4	0.00	96.83	1.79	1.39	3.17	0.242
OA-0209-TP5	0.41	87.15	7.11	5.33	12.44	0.120
OA-0209-TP6	0.21	89.72	6.72	3.36	10.08	0.318

Table 13. Sediment Sample Composition Information.

USGS Sample Identifier	Component Analyzed	Total Inorganic carbon [percent]	Calcium Carbonate [percent]]	Terrigenous [percent]
OA-0209-SF2	Bulk	11.08	92.31	7.69
OA-0209-SF3	Bulk	11.40	94.94	5.06
OA-0209-SF4	Bulk	11.42	95.15	4.85
OA-0209-SF5	Bulk	11.33	94.36	5.64
OA-0209-SF6	Bulk	11.52	95.98	4.02
OA-0209-TP2	Bulk	10.81	90.03	9.97
OA-0209-TP3	Bulk	8.72	72.64	27.36
OA-0209-TP4	Bulk	11.34	94.43	5.57
OA-0209-TP5	Bulk	10.63	88.55	11.45
OA-0209-TP6	Bulk	10.22	85.13	14.87
OA-0209-SF2	Sand	11.20	93.26	6.74
OA-0209-SF3	Sand	11.50	95.82	4.18
OA-0209-SF4	Sand	11.56	96.34	3.66
OA-0209-SF5	Sand	11.59	96.52	3.48
OA-0209-SF6	Sand	11.68	97.31	2.69
OA-0209-TP2	Sand	11.23	93.55	6.45
OA-0209-TP3	Sand	11.33	94.38	5.62
OA-0209-TP4	Sand	11.29	94.08	5.92
OA-0209-TP5	Sand	11.34	94.46	5.54
OA-0209-TP6	Sand	11.56	96.31	3.69
OA-0209-TP2	Silt*	10.18	84.82	15.18
OA-0209-TP3	Silt*	10.46	87.16	12.84
OA-0209-TP4	Silt*	10.38	86.49	13.51
OA-0209-TP5	Silt*	10.26	85.46	14.54
OA-0209-TP6	Silt*	10.19	84.88	15.12
OA-0209-TP2	Clay*	9.64	80.33	19.67
OA-0209-TP3	Clay*	7.98	66.45	33.55
OA-0209-TP4	Clay*	9.01	75.04	24.96
OA-0209-TP5	Clay*	8.63	71.85	28.15
OA-0209-TP6	Clay*	7.95	66.18	33.82

*The seabed sediment samples had insufficient silt and clay fractions for geochemical analyses.

Table 14. Sediment Flux Statistics

All statistics were calculated for 2008 Year Days 315-325.

Site Name	Depth [m]	Sediment Flux [kg/cm^2]	Direction [degrees]
MP2	20	1.60	148
MP3	20	5.60	136
MP4	9	25.06 [1468.00]*	117 [116]*
MP5	9	52.48 [2680.05]*	113 [132]*
MP6	8	4.50 [519.03]*	125 [117]*

*Additional statistics were calculated for 2008 Year Days 315-396.

Appendixes

Appendix 1
ADCP Information

RD Instruments 600 kHz Workhorse Monitor upward-looking acoustic Doppler current profiler
s/n: 2074, 2432, 7449

Transmitting Frequency:	614 kHz
Depth of Transducer:	20 m
Blanking Distance:	0.25 m
Height of First Bin above Bed:	1.11 m
Bin Size:	0.5 m
Number of Bins:	48
Operating Mode:	High-resolution, broad bandwidth
Sampling Frequency:	2 Hz
Time per Ping:	00:03.00
Pings per Ensemble:	100
Profile Ensemble Interval:	0:10:00.00
Wave Ensemble Interval:	2:00:00.00
Sound Speed Calculation:	Set salinity, updating temperature via sensor

Nortek Instruments 2 MHz Aquadopp upward-looking acoustic Doppler current profiler
s/n: 1862, 1851

Transmitting Frequency:	2000 kHz
Depth of Transducer:	10 m
Blanking Distance:	0.25 m
Height of First Bin above Bed:	0.75 m
Bin Size:	0.50 m
Number of Bins:	20
Average interval:	0:02:00.00
Profile interval:	0:10:00.00
Wave interval:	1:00:00.00
Wave cell size:	2 m
Operating Mode:	High-resolution
Sound Speed Calculation:	Set salinity, updating temperature via sensor

Nortek Instruments 600 kHz AWAC upward-looking acoustic Doppler current profiler
s/n: 5461

Transmitting Frequency:	600 kHz
Depth of Transducer:	20 m
Blanking Distance:	0.25 m
Height of First Bin above Bed:	0.75 m
Bin Size:	0.50 m
Number of Bins:	20
Average interval:	0:02:00.00
Profile interval:	0:10:00.00
Wave interval:	1:00:00.00
Wave cell size:	2 m
Operating Mode:	High-resolution
Sound Speed Calculation:	Set salinity, updating temperature via sensor

Data Processing:

The RDI current data were processed using the WinADCP program and the wave data using the WavesMon program. The Nortek current data were processed using the Prof2NDP program and the wave data using the QuickWave program.

The data were averaged over 1 hour ensembles, all of the spurious data above the water surface were removed and all of the data in bins where the beam correlation dropped below 80% were removed for visualization and analysis.

Appendix 2
CT and SLOBS Information

Seabird Microcat SBE-37SM temperature-conductivity (CT) sensors
s/n: 3800, 3801, 4087, 4089, 4368, and 4369

Sampling Frequency:	2 Hz
Measurements per Burst:	8
Time Between Bursts:	00:05:00.00

Aquatec/Seapoint 200-TY self-logging optical backscatter sensors (SLOBS)
s/n: 371-013, 371-026

Aquatec/Seapoint 210-TYT self-logging optical backscatter sensors (SLOBS)
s/n: 024-002, 024-005, 024-006, 024-007

Sampling Frequency:	2 Hz
Measurements per Burst:	8
Time Between Bursts:	00:05:00.00

Data Processing:

The CT and SLOBS data were post-processed for visualization and analysis by removing all instantaneous (only one data point in time) data spikes that exceeded the deployment mean + 3 standard deviations.

Appendix 3
WS, CIS, and TIS Information

NovaLynx WS-16N-A Marine-grade Weather Station:

Anemometer:	200-05106-MA (marine model)
Temperature & Relative Humidity:	110-WS-16TH-A w/radiation shield
Barometric Pressure Sensor:	110-WS-16BP
Rain Gauge:	110-WS-16RC
Sampling Frequency:	1 Hz
Measurements per Burst:	1800
Time Between Bursts:	00:30:00.00

USGS Terrestrial Imaging System:

Camera:	Nikon CoolPix 8700 8-megapixel digital camera
Programmable Automated Controller:	Campbell Scientific Scientific CR200
Sampling Times:	06:00, 07:00, 08:00, 10:00, 12:00, 14:00, 16:00, and 18:00 HST

USGS Coral Imaging System

Camera:	Nikon CoolPix 8700 8-megapixel digital camera
Programmable Automated Controller:	Campbell Scientific Scientific CR200
Sampling Times:	00:00, 04:00, 08:00, 12:00, 16:00, and 20:00 HST

Appendix 4
Water Column Profiler Information

Conductivity/Temperature/Depth (CTD) Profiler with Optical Backscatter (OBS), Photosynthetically-Available Radiation (PAR), Dissolved Oxygen (DO), and Chlorophyll (chl) Sensors

Instruments:

Seabird 19plus CTD sensor; s/n:	4299
D&A Instruments OBS-3 sensor; s/n:	19830-2000
Licor #II-193SA PAR sensor; s/n:	SPQA-3562
Seabird SBE 43 oxygen sensor; s/n:	430731
Wet Labs 9502016 fluorometer; s/n:	WS3-017, 0-75 ug/l
Sampling Frequency:	4 Hz

Position Information:

Garmin GPS-76 GPS; s/n: 80207465; USGS/CRP unit#1

Data Processing:

The profiler data were processed using the SBE Data Processing program.

The data were averaged into 0.5 m vertical bins and all of the spurious data marked by a flag in the raw data were removed for visualization and analysis. Stratification were measured as the difference between the mean of the top three bins (0.5-1.5 m below the surface) and the bottom three bins (0.5-1.5 m above the bed).

Appendix 5
Water column profiler log: November 2008

Cast Number/Site	Date	Time [HST]	Latitude [decimal degrees]	Longitude [decimal degrees]	Depth [m]
1	11/09/2008	07:50	-157.79839	21.24416	19.6
2	11/09/2008	08:15	-157.74876	21.25575	19.0
3	11/09/2008	08:33	-157.71508	21.25974	19.8
4	11/09/2008	08:39	-157.71798	21.26610	8.1
5	11/09/2008	09:04	-157.72517	21.27300	5.1
6	11/09/2008	09:10	-157.72991	21.26546	14.1
7	11/09/2008	09:18	-157.71614	21.27097	5.0
8	11/09/2008	09:22	-157.71457	21.27447	1.6
9	11/09/2008	09:26	-157.71372	21.27645	4.9
10	11/09/2008	09:29	-157.71306	21.27780	4.5
11	11/09/2008	09:31	-157.71339	21.27885	3.9
12	11/09/2008	09:34	-157.71181	21.28121	1.8
13	11/09/2008	09:47	-157.73419	21.27342	7.4
14	11/09/2008	09:55	-157.74914	21.27110	6.5
15	11/09/2008	10:01	-157.75034	21.26324	14.5
16	11/09/2008	10:08	-157.76058	21.26740	6.7
17	11/09/2008	10:16	-157.77426	21.26371	7.0
18	11/09/2008	10:22	-157.77305	21.25686	14.8
19	11/09/2008	10:30	-157.78619	21.25718	7.3
20	11/09/2008	10:40	-157.79980	21.25111	10.5
21	11/09/2008	10:43	-157.80019	21.24799	12.4

Appendix 6
Water column profiler log: February 2009

Cast Number/Site	Date	Time [HST]	Latitude [decimal degrees]	Longitude [decimal degrees]	Depth [m]
1	02/20/2009	07:54	-157.79820	21.24400	19.9
2	02/20/2009	08:01	-157.80016	21.24809	12.2
3	02/20/2009	08:05	-157.79985	21.25112	9.5
4	02/20/2009	08:21	-157.77017	21.25021	21.3
5	02/20/2009	08:33	-157.74876	21.25558	19.5
6	02/20/2009	08:42	-157.73181	21.25807	18.6
7	02/20/2009	08:53	-157.71502	21.25971	19.8
8	02/20/2009	09:00	-157.71805	21.26598	7.9
9	02/20/2009	09:05	-157.71607	21.27085	4.9
10	02/20/2009	09:09	-157.71440	21.27455	0.9
11	02/20/2009	09:12	-157.71360	21.27632	4.6
12	02/20/2009	09:15	-157.71305	21.27774	4.3
13	02/20/2009	09:19	-157.71338	21.27884	3.7
14	02/20/2009	09:23	-157.71180	21.28114	1.7
15	02/20/2009	09:34	-157.72521	21.27286	5.5
16	02/20/2009	09:40	-157.73001	21.26533	14.0
17	02/20/2009	09:47	-157.73428	21.27334	7.3
18	02/20/2009	09:55	-157.74930	21.27100	6.1
19	02/20/2009	10:00	-157.75042	21.26298	14.9
20	02/20/2009	10:07	-157.76071	21.26722	8.2
21	02/20/2009	10:15	-157.77315	21.25671	14.3
22	02/20/2009	10:22	-157.77450	21.26349	9.5
23	02/20/2009	10:29	-157.78641	21.25703	8.2

Appendix 7
Suspended Sediment Concentration (SSC) Calibration Information

Sample/Site	Filter mass, initial (g)	Sample volume (l)	Filter mass, final (g)	Sediment mass (g)	Concentration (mg/l)	OBS, observed (N.T.U.)	OBS, corrected (N.T.U.)
MB-1	0.096	0.558	0.104	0.008	14.34	30	2
MB-2	0.098	0.561	0.191	0.093	165.78	41	13
MB-3	0.097	0.568	0.468	0.371	653.17	105	77